

Article

Identification of Differential Compositions of Aqueous Extracts of Cinnamomi Ramulus and Cinnamomi Cortex

Pei Wang^{1,2,†}, Jun Chi^{1,2,†}, Hui Guo^{1,2}, Shun-Xiang Wang^{1,2}, Jing Wang^{1,2}, Er-Ping Xu^{1,2}, Li-Ping Dai^{1,2,*} and Zhi-Min Wang^{2,3,*} 

¹ Henan University of Chinese Medicine, Zhengzhou 450046, China

² Engineering Technology Research Center for Comprehensive Development and Utilization of Authentic Medicinal Materials in Henan Province, Henan University of Chinese Medicine, Zhengzhou 450046, China

³ National Engineering Laboratory for Quality Control Technology of Chinese Herbal Medicines, Institute of Chinese Materia Medica, China Academy of Chinese Medical Sciences, Beijing 100700, China

* Correspondence: liping_dai@hactcm.edu.cn (L.-P.D.); zhmw123@163.com (Z.-M.W.);
Tel.: +86-187-0365-1652 (L.-P.D.)

† These authors contributed equally to this work.

Abstract: Cinnamomi ramulus (CR) and Cinnamomi cortex (CC), both sourced from *Cinnamomum cassia* Presl, are commonly used Chinese medicines in the Chinese Pharmacopeia. However, while CR functions to dissipate cold and to resolve external problems of the body, CC functions to warm the internal organs. To clarify the material basis of these different functions and clinical effects, a simple and reliable UPLC-Orbitrap-Exploris-120-MS/MS method combined with multivariate statistical analyses was established in this study with the aim of exploring the difference in chemical compositions of aqueous extracts of CR and CC. As the results indicated, a total of 58 compounds was identified, including nine flavonoids, 23 phenylpropanoids and phenolic acids, two coumarins, four lignans, four terpenoids, 11 organic acids and five other components. Of these compounds, 26 significant differential compounds were identified statistically including six unique components in CR and four unique components in CC. Additionally, a robust HPLC method combined with hierarchical clustering analysis (HCA) was developed to simultaneously determine the concentrations and differentiating capacities of five major active ingredients in CR and CC: coumarin, cinnamyl alcohol, cinnamic acid, 2-methoxycinnamic acid and cinnamaldehyde. The HCA results showed that these five components could be used as markers for successfully distinguishing CR and CC. Finally, molecular docking analyses were conducted to obtain the affinities between each of the abovementioned 26 differential components, focusing on targets involved in diabetes peripheral neuropathy (DPN). The results indicated that the special and high-concentration components in CR showed high docking scores of affinities with targets such as HbA1c and proteins in the AMPK–PGC1–SIRT3 signaling pathway, suggesting that CR has greater potential than CC for treating DPN.

Keywords: Cinnamomi ramulus; Cinnamomi cortex; LC-MS; multivariate statistical analysis; quantitative analysis; molecular docking



Citation: Wang, P.; Chi, J.; Guo, H.; Wang, S.-X.; Wang, J.; Xu, E.-P.; Dai, L.-P.; Wang, Z.-M. Identification of Differential Compositions of Aqueous Extracts of Cinnamomi Ramulus and Cinnamomi Cortex. *Molecules* **2023**, *28*, 2015. <https://doi.org/10.3390/molecules28052015>

Academic Editor: Thomas Letzel

Received: 12 January 2023

Revised: 16 February 2023

Accepted: 18 February 2023

Published: 21 February 2023



Copyright: © 2023 by the authors. Licensee MDPI, Basel, Switzerland. This article is an open access article distributed under the terms and conditions of the Creative Commons Attribution (CC BY) license (<https://creativecommons.org/licenses/by/4.0/>).

1. Introduction

Cinnamomi ramulus (CR, *Guizhi* in Chinese) and Cinnamomi cortex (CC, *Rougui* in Chinese), are, respectively, the dried twigs and bark of *Cinnamomum cassia* Presl. They are documented in the Chinese Pharmacopoeia, which has a long history and comprises all well-known Chinese medicines with a high clinical value [1]. CR functions to dissipate wind-cold and resolve external problems of the body; it traverses the arms and warms the meridians. It is known as the first medicine of classic prescription and is widely used in the Treatise on Cold Pathogenic and Miscellaneous Diseases [2]. In contrast, CC functions to warm the internal organs, nourish and warm kidney-yang, dispel cold, and relieve pain. Different pharmacological effects result from variant chemical ingredients. It can be

assumed that several significant components differ in CR and CC, leading to differences in their respective efficacies. Previous chemical investigations demonstrated that CR and CC contained various compositions, including phenylpropanoids, phenolic acids, flavonoids and terpenoids and so on [3–5]. A previous study showed that the contents of volatile oils in CR and CC, were 0.15% and 0.31%, respectively, with the main component being cinnamaldehyde [6]. The traditional usage of decocting with water requires that it is necessary to continue to analyze the different components of the aqueous extracts of CR and CC.

In this study, a simple, rapid, valid, and reliable UPLC-Orbitrap-Exploris-120-MS/MS [7–10] method was developed to assess the difference in the chemical compositions of CR and CC. By comparing the MS/MS information of the detected compounds with the mass spectrometry database, records in the literature, and standard references, 58 compounds were preliminary identified. Eight batches of CR and CC samples were comparatively analyzed using this method coupled with multivariate statistical analysis [11–13]. As a result, 26 statistically significant ($p < 0.05$) discrepant compounds were characterized. Additionally, a robust HPLC method combined with hierarchical clustering analysis (HCA) was developed to simultaneously determine the concentrations and differentiating capacities of five major active ingredients in CR and CC: coumarin, cinnamyl alcohol, cinnamic acid, 2-methoxycinnamic acid and cinnamaldehyde. The HCA results showed that *trans*-cinnamaldehyde and cinnamyl alcohol could be used as markers to successfully distinguish CR and CC.

Diabetes peripheral neuropathy (DPN), one of the most common complications of diabetes mellitus, is commonly categorized as Xiaoke (diabetes) complicated by arthralgia syndrome in TCM [14]. As a diaphoretic, CR functions to dissipate wind-cold and is usually used for treating arthralgia syndrome caused by rheumatoid arthritis and diabetes [15,16]. CR is always included in TCM formulars for treating DPN, e.g., *Huangqi Guizhi Wuwu Decoction* [17,18]. In clinics, HbA1c is used as an essential indicator to evaluate the severity of DPN [19,20]. As a vital signaling pathway, AMPK–PGC1–SIRT3 was widely reported and involved in the occurrence and development of DPN [21]. Using virtual molecular docking technology, we, therefore, explored whether any ingredients occurring in CR are different from those in CC and, if so, whether they contribute to anti-DNP activities. The findings of this study will provide comparative information on the chemical profiles of CR and CC and lay the groundwork for exploring effective CR substances as anti-DNP agents.

2. Results and Discussion

2.1. Optimization of the LC-MS Conditions

In order to improve the sensitivity and resolution of the analysis but reduce analytical time, the LC-MS conditions for aqueous extract of CR, which included mobile phase, flow rate, column temperature, ion mode and ion source parameters, were optimized. First, methanol/0.1% formic acid water and acetonitrile/0.1% formic acid water were investigated to achieve better separation. It was found that acetonitrile/0.1% formic acid water was the most suitable to obtain more peak and better peak shape. Second, we compared two types of columns (Waters Acquity UPLC BEH C18 and HYPERSILGOLD Vanquish C18) and found that the latter column had better resolution and more peaks. Different column temperatures (25 and 35 °C) were tested and a good separation effect and higher peak intensity was obtained for the constituents at 35 °C. In addition, we also compared the vaporizer temperature (320 and 350 °C) and the positive ion spray voltage (3.8 and 3.5 kV), and finally we found that the TIC had high sensitivity and good resolution when the vaporizer temperature was 350 °C and the positive ion spray voltage was 3.5 kV. The above data are shown in Table S1.

2.2. Identification of the Constituents of CR and CC

Qualitative analysis of the chemical constituents of the aqueous extracts of CR and CC was performed using UPLC-Orbitrap-Exploris-120-MS/MS, in both in the positive

and negative modes. In the qualitative analysis, in order to evaluate the stability of the instrument, mixed standards (QC) were repeated for 8 times. The RSD_5 of the retention times and intensities in QC samples were all less than 5%. Typical total ion chromatograms for CR and CC, both in negative ion mode are shown in Figure S1. A comparison of retention times, accurate mass, fragmentation patterns, and a comparison with an online database, as well as referencing to the related literature to validate the data, preliminarily identified 58 compounds (Table 1, Figures S2 and S3); these included nine flavonoids, 23 phenylpropanoids and phenolic acids, two coumarins, four lignans, four terpenoids, 11 organic acids and five other components. Among these compounds, eight compounds were identified by comparing their retention times, characteristic molecular ions, and fragment ions to those of the standards (Figure S4). Significantly, among these compounds, 26 significant differential compounds were identified statistically: the results showed that the peak areas of flavonoids and flavonoid glycosides, and phenylpropanoids except cinnamaldehyde and cinnamyl alcohol in CR were higher than in CC, and the peak areas of terpenoids and organic acids in CC were higher than in CR.

2.2.1. Identification of Phenylpropanoids and Phenolic Acids

Phenylpropanoids and phenolic acids are major bioactive constituents in CR and CC [22]. *Trans*-cinnamic acid, *trans*-cinnamaldehyde, cinnamyl alcohol and 2-methoxycinnamic acid were shown to be the main phenylpropanoids. In the literature, the diagnostic ions at m/z 163/165, 151/153 and 135/137 105/107 were indicators of phenylpropanoids and phenolic acids [23]. However, in addition to the above diagnostic ions reported in the literature and standards, our statistical analysis found that fragment ions at m/z 105/107 and 123/125 can also be diagnostic ions [23].

With the transfer of electrons, the carbonyl group was also prone to cleavage and the loss of CO and CH₂ to form fragment ion peaks [24,25]. As a result, when compared to the diagnostic ions described above, the mass spectra of the standards, fragmentation information in the database and previously reported fragmentation spectra, a total of 23 phenylpropanoids and phenolic acids were identified in CR and CC. Compounds 45 and 48 were chosen as typical examples to illustrate the fragmentation pathways.

The molecular ion peak m/z 149.0231 [M + H]⁺ was obtained in the ESI (+) mode for compound 45, which had the molecular formula C₉H₈O₂ and a relative molecular mass of 148.0525. The matching fragments were m/z 131.0493 [M – H₂O + H]⁺ and m/z 105.0539 [M – CO + H]⁺ (Table 1), which were in general agreement with the literature and data available for cinnamic acid; accordingly, the compound was presumed to be *trans*-cinnamic acid [26]. The MS² spectrum of compound 45 is shown in Figure S5 and the possible cleavage process of the positive ions is shown in Figure 1.

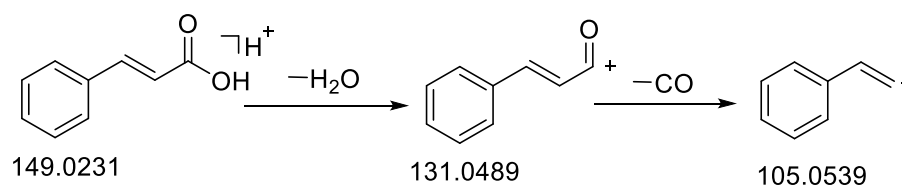


Figure 1. Fragmentation pathway of *trans*-cinnamic acid in positive ion mode.

Table 1. Identification of chemical constituents in CR and CC.

NO.	Name	RT	Formula	Calc. MW	Error (ppm)	Theoretical Mass (m/z)	Experimental Mass (m/z)	MS ² (m/z)	Total Score (%) ^a	Ref.	Source ^b
1	Gentisic acid-5-O-glucoside	3.15	C ₁₃ H ₁₆ O ₉	316.0781	-0.50	315.0711 [M - H] ⁻	315.0709 [M - H] ⁻	270.8695 [M - COOH + H] ⁺ , 165.0183, 153.0185 [M - C ₆ H ₁₀ O ₅ + H] ⁺ , 152.0108, 113.0240, 109.0293 [M - C ₆ H ₁₀ O ₅ - COOH + H] ⁺ , 108.0211	91.2	[27]	
2	Isovanillic acid	3.22	C ₈ H ₈ O ₄	168.0415	1.88	167.0339 [M - H] ⁻	167.0342 [M - H] ⁻	152.0116 [M - CH ₃ - H] ⁻ , 151.0226 [M - OH] ⁻ , 123.0449 [M - COOH - H] ⁻ , 108.0217 [M - COOH - CH - H] ⁻		[28–30]	CR, <i>C. cassia</i> leaves
3	Gentisic acid	3.30	C ₇ H ₆ O ₄	154.0257	3.04	153.0182 [M - H] ⁻	153.0187 [M - H] ⁻	153.0187 , 135.0182 [M - H ₂ O + H] ⁺ , 109.0288 [M - COOH + H] ⁺ , 85.0289, 81.0343 [M - COOH - CO + H] ⁺ , 68.9978	96.6	[31,32]	<i>C. cassia</i>
4	Syringic acid	3.65	C ₉ H ₁₀ O ₅	198.0527	-4.53	199.0601 [M + H] ⁺	199.0588 [M + H] ⁺	181.0495 [M - OH + H] ⁺ , 163.1478 [M - 2H ₂ O + H] ⁺ , 155.0166, 153.0764 [M - OH - OCH ₃ + H] ⁺ , 95.0492	75.3	[31]	CR, CC, <i>C. cassia</i> leaves
5	Catechol	3.80	C ₆ H ₆ O ₂	110.0363	4.05	109.0284 [M - H] ⁻	109.0291 [M - H] ⁻	108.0215 [M - 2H] ⁻ , 93.7792 [M - OH - H] ⁻ , 81.6772	97.4	[33]	CR
6	Neochlorogenic acid	4.40	C ₁₆ H ₁₈ O ₉	354.0936	-4.21	353.0892 [M - H] ⁻	353.0886 [M - H] ⁻	191.0550 [M - C ₉ H ₆ O ₃ - H] ⁻ , 179.0343 [M - C ₇ H ₁₀ O ₅ - H] ⁻ , 161.0237 [M - C ₇ H ₁₀ O ₅ - H ₂ O - H] ⁻ , 135.0445 [M - C ₇ H ₁₀ O ₅ - CO ₂ - H] ⁻ , 111.0446		[34]	CR, CC
7	Salicylic acid	5.38	C ₇ H ₆ O ₃	138.0311	3.50	137.0233 [M - H] ⁻	137.0238 [M - H] ⁻	119.0132 [M - H ₂ O - H] ⁻ , 108.8992 [M - CO - H] ⁻ , 93.0343 [M - COO - H] ⁻	62.9	[31,35]	CR, CC
8	Citrinin	5.40	C ₁₃ H ₁₄ O ₅	250.0840	-0.46	251.0916 [M + H] ⁺	251.0915 [M + H] ⁺	233.0804 [M - H ₂ O + H] ⁺ , 221.0807 [M - 2CH ₃ + H] ⁺ , 205.0857 [M - H ₂ O - CO + H] ⁺ , 204.0785, 191.0701	75.5		
9	4-Methoxy benzaldehyde	6.30	C ₈ H ₈ O ₂	136.0523	-0.77	137.0597 [M + H] ⁺	137.0596 [M + H] ⁺	122.0362 [M - CH ₃ + H] ⁺ , 107.0490 [M - OCH ₂ + H] ⁺ , 93.0590 [M - CO - CH ₃ + H] ⁺ , 91.0543, 81.0698, 79.0543 [M - CO - OCH ₃ + H] ⁺	81.9	[28,36]	CR, CC, <i>C. cassia</i> leaves
10	Darendoside A	6.32	C ₁₉ H ₂₈ O ₁₁	432.1613	-2.29	431.1547 [M - H] ⁻	431.1538 [M - H] ⁻	191.0547, 161.0446, 149.0447, 113.0245, 99.0081, 89.0244	67.5		
11	Epicatechin	8.41	C ₁₅ H ₁₄ O ₆	290.0788	-1.08	291.0863 [M + H] ⁺	291.0860 [M + H] ⁺	273.0768 [M - H ₂ O + H] ⁺ , 249.0766 , 179.0340 [M - C ₆ H ₆ O ₂ + H] ⁺ , 165.0544 [M - C ₆ H ₆ O ₂ - CH ₂ + H] ⁺ , 151.0394, 139.0388 [M - C ₉ H ₁₁ O ₂ + H] ⁺ , 125.0239 [M - C ₉ H ₈ O ₃ + H] ⁺ , 123.0439 , 119.0491, 109.0290 [M - C ₉ H ₁₀ O ₄ + H] ⁺ , 95.0490	99.4	Standard, [37]	CR

Table 1. Cont.

NO.	Name	RT	Formula	Calc. MW	Error (ppm)	Theoretical Mass (m/z)	Experimental Mass (m/z)	MS ² (m/z)	Total Score (%) ^a	Ref.	Source ^b
12	2,4,6-Trihydroxy-2-(4-hydroxybenzyl)-1-benzofuran-3(2H)-one	8.68	C ₁₅ H ₁₂ O ₆	288.0621	−4.34	287.0521 [M − H] [−]	287.0511 [M − H] [−]	161.0233 [M − C ₆ H ₆ O ₃ − H] [−] , 131.2500, 125.0239 [M − C ₈ H ₂ O ₄ − H] [−]	88.7		
13	Dihydrophaseic acid	8.75	C ₁₅ H ₂₂ O ₅	282.1454	−0.53	281.1383 [M − H] [−]	281.1382 [M − H] [−]	237.1486 [M − CHO − H] [−] , 201.1273 [M − CHO − H ₂ O − OH − H] [−] , 189.1278, 171.1171, 139.0758	76.8		
14	Catechin	8.83	C ₁₅ H ₁₄ O ₆	290.0777	−1.26	289.0707 [M − H] [−]	289.0703 [M − H] [−]	289.0703 [M − H ₂ O − H] [−] , 271.0603, 245.08081, 203.07036, 151.0393, 125.0239, 109.0290		[35]	CC
15	Vanillin	9.28	C ₈ H ₈ O ₃	152.0472	−0.82	153.0548 [M + H] ⁺	153.0545 [M + H] ⁺	153.0545 , 125.0595 [M − CO + H] ⁺ , 111.0441, 93.0333, 65.0387	90.7	[28,31,38]	<i>C. cassia</i> leaves
16	4-Acetyl-3-hydroxy-5-methylphenyl-β-D-glucopyranoside	10.08	C ₁₅ H ₂₀ O ₈	328.1144	−1.05	327.1074 [M − H] [−]	327.1071 [M − H] [−]	165.0547 [M − C ₆ H ₁₀ O ₅ − H] [−] , 147.0446 [M − C ₆ H ₁₀ O ₅ − H ₂ O − H] [−] , 121.0653 [M − C ₆ H ₁₀ O ₅ − OH − CH ₃ − CH ₂ − OH] [−] , 106.0416	91.7	[27]	
17	Picconioside B	10.95	C ₂₆ H ₄₀ O ₁₂	544.2500	−3.66	543.2438 [M − H] [−]	543.2421 [M − H] [−]	525.2305 [M − H ₂ O − H] [−] , 363.1800 [M − H ₂ O − C ₆ H ₁₀ O ₅ − H] [−] , 381.1912, 167.1070, 165.0922, 101.0240, 89.0240, 59.0136	91.2		
18	2-Methoxybenzoic acid	12.68	C ₈ H ₈ O ₃	152.0472	−0.92	153.0546 [M + H] ⁺	153.0545 [M + H] ⁺	153.0545 , 135.0439, 111.0440, 105.0441, 95.0491 [M − CO ₂ − CH ₂ + H] ⁺ , 93.0699, 79.0541	96.3	[39,40]	CR
19	Taxifolin	13.79	C ₁₅ H ₁₂ O ₇	304.0581	2.03	305.0656 [M + H] ⁺	305.0662 [M + H] ⁺	287.0573 [M − H ₂ O + H] ⁺ , 259.0591 [M − CO − H ₂ O + H] ⁺ , 231.0652 , 153.0188 [M − CO − C ₇ H ₈ O ₂ + H] ⁺ , 149.0230	91.1	Standard, [12,41]	CR
20	Lyoniresinol-3a-O-β-D-glucopyranosid	13.89	C ₂₈ H ₃₈ O ₁₃	582.2289	−4.09	581.2230 [M − H] [−]	581.2209 [M − H] [−]	566.1975, 535.1785, 419.1691 [M − C ₆ H ₁₀ O ₅ − H] [−] , 404.1459, 373.1275 [M − C ₆ H ₁₀ O ₅ − 3CH ₃ − H] [−] , 359.1110 [M − C ₆ H ₁₀ O ₅ − 4CH ₃ − H] [−] , 233.0812, 202.0624, 153.0549, 138.0316 [M − C ₆ H ₁₀ O ₅ − OH − C ₁₄ H ₁₈ O ₆ − H] [−] , 101.0238	92.3	[33,42,43]	CC
21	4-Ethylphenol	14.12	C ₈ H ₁₀ O	122.0726	4.32	121.0649 [M − H] [−]	121.0654 [M − H] [−]	106.0419 [M − CH ₃ − H] [−] , 90.9232 [M − CH ₃ − O − H] [−] , 61.9880	87.9	[44,45]	<i>C. cassia</i>
22	(−)-Lyoniresinol	14.19	C ₂₂ H ₂₈ O ₈	420.1766	−1.53	419.1700 [M − H] [−]	419.1694 [M − H] [−]	373.1277 [M − 3CH ₃ − H] [−] , 359.1119 [M − 4CH ₃ − H] [−] , 313.0712, 221.0801, 180.0404, 139.0396, 134.0383	96.0	[33]	

Table 1. Cont.

NO.	Name	RT	Formula	Calc. MW	Error (ppm)	Theoretical Mass (m/z)	Experimental Mass (m/z)	MS ² (m/z)	Total Score (%) ^a	Ref.	Source ^b
23	Lyoniside	14.33	C ₂₇ H ₃₆ O ₁₂	552.2186	−3.79	551.2123 [M − H] [−]	551.2105 [M − H] [−]	536.1875, 419.1650, 389.1591, 374.1359, 373.1275 [M − C ₆ H ₁₀ O ₅ − 3CH ₃ − H] [−] , 359.1105 [M − C ₆ H ₁₀ O ₅ − 4CH ₃ − H] [−] , 341.1013, 325.1092, 233.0823, 119.0345, 113.0239	91.8	[33]	
24	3-Oxoindane-1-carboxylic acid	14.41	C ₁₀ H ₈ O ₃	176.0472	−0.69	177.0546 [M + H] ⁺	177.0545 [M + H] ⁺	153.9367, 149.0596 [M − CO + H] ⁺ , 133.0646 [M − COO + H] ⁺ , 131.0490, 121.1010, 107.0490, 105.0693 [M − CO − COO + H] ⁺ , 93.0098 [M − CO − COO − C + H] ⁺ , 81.0700 [M − CO − COO − 2C + H] ⁺	72.2		
25	3-Methoxy phenylacetic acid	14.52	C ₉ H ₁₀ O ₃	166.0622	1.69	165.0546 [M − H] [−]	165.0549 [M − H] [−]	147.0443, 136.9315 [M − OCH ₃ − H] [−] , 121.0654, 106.0419, 96.9597 [M − C ₂ H ₅ O ₂ − H] [−]		[39]	
26	2-(4-Hydroxyphenyl)-7-((3,4,5-trihydroxy-6-(hydroxymethyl) tetrahydro-2H-pyran-2-yl) oxy) chroman-4-one	14.53	C ₂₁ H ₂₂ O ₉	418.1248	−0.74	417.1180 [M − H] [−]	417.1177 [M − H] [−]	301.0338 [M − C ₆ H ₁₀ O ₅ − H] [−] , 255.0651, 153.0187 [M − C ₆ H ₁₀ O ₅ − CO − C ₇ H ₆ O ₂ − H] [−] , 135.0082 [M − C ₆ H ₁₀ O ₅ − CO − C ₇ H ₆ O ₂ − H ₂ O − H] [−] , 119.0497, 91.0184	67.5	[12]	
27	Quercetin-3β-D-glucoside	14.55	C ₂₁ H ₂₀ O ₁₂	464.0936	0.21	463.0871 [M − H] [−]	463.0872 [M − H] [−]	301.0338 [M − H − C ₆ H ₁₀ O ₅] [−] , 300.0270, 271.0247		[34]	
28	2-[1-(2H-1,3-Benzodioxol-5-yl)propan-2-yl]-6-methoxy-4-(prop-2-en-1-yl)phenol	14.74	C ₂₀ H ₂₂ O ₄	326.1516	0.63	327.1590 [M + H] ⁺	327.1593 [M + H] ⁺	312.1348, 295.1328 [M − OCH ₂ + H] ⁺ , 280.1095, 263.1071, 251.0001, 235.1122, 175.0758, 163.0753 [M − C ₁₀ H ₁₂ O ₂ + H] ⁺ , 151.075, 137.0596, 133.0647, 103.0540, 98.9841	71.6		
29	Cinnamylalcohol-6'-O-α-furanarabinose-O-β-glucopyranoside	14.81	C ₂₀ H ₂₈ O ₁₀	428.1664	−4.38	427.1598 [M − H] [−]	427.1582 [M − H] [−]	293.0861, 233.0650, 191.0549, 161.0451, 149.0448, 125.0239, 89.0240, 81.0344, 59.0136	85.9	[46]	CR
30	6-Methoxymellein	14.99	C ₁₁ H ₁₂ O ₄	208.0734	−0.55	209.0804 [M + H] ⁺	209.0802 [M + H] ⁺	191.0701, 181.0847, 177.0544, 163.0765, 149.0596 [M − COOCH + H] ⁺ , 131.0486, 121.0647 [M − 2OH − OCH ₃ − CO + H] ⁺ , 109.0647, 103.0540, 93.0698, 91.0540, 55.0177	85.8		

Table 1. Cont.

NO.	Name	RT	Formula	Calc. MW	Error (ppm)	Theoretical Mass (m/z)	Experimental Mass (m/z)	MS ² (m/z)	Total Score (%) ^a	Ref.	Source ^b
31	Coumarin	15.18	C ₉ H ₆ O ₂	146.0366	−1.33	147.0441 [M + H] ⁺	147.0439 [M + H] ⁺	127.0543, 103.0541 [M − CO ₂ + H] ⁺ , 91.0540 [M − 2CO + H] ⁺ , 43.0242 303.0496 , 275.0399 [M − CO + H] ⁺ , 257.0446 [M − CO − H ₂ O + H] ⁺ , 247.0590, 229.0491 [M − 2CO − H ₂ O + H] ⁺ , 199.0434 [M − 3CO − H ₂ O + H] ⁺ , 165.0178 , 163.0389, 153.0183 [M − CO − C ₇ H ₆ O ₂ + H] ⁺ , 133.0231 [M − CO − C ₇ H ₄ O ₂ − H ₂ O + H] ⁺ , 121.0297, 111.0075 431.0983, 369.0594, 345.0606, 315.0494, 303.0497 [M + H − C ₆ H ₉ O ₄] ⁺ , 257.0439 [M − C ₆ H ₉ O ₄ − CO − H ₂ O + H] ⁺ , 229.0492 [M − C ₆ H ₉ O ₄ − 2CO − H ₂ O + H] ⁺ , 129.0548, 85.0283, 71.0490 476.1080, 417.1531 [M − C ₆ H ₁₀ O ₅ − H] [−] , 300.0259 [M − C ₆ H ₈ O ₄ − C ₅ H ₁₀ O ₄ − H] [−] , 271.0235 [M − C ₁₁ H ₁₆ O ₁₀ − H] [−] , 178.9979 [M − C ₁₇ H ₂₀ O ₁₁ − H] [−] 313.1796 [M − H ₂ O + H] ⁺ , 295.1676, 271.1686, 243.1763, 165.0911, 125.0565 [M − C ₁₂ H ₁₄ O ₃ + H] ⁺ 255.1391 [M − H ₂ O + H] ⁺ , 245.1534, 227.1441 [M − H ₂ O − CO + H] ⁺ , 203.1070, 149.0964 [M − CH ₃ − C ₆ H ₆ O ₂ + H] ⁺ , 82.8045 [M − C ₁₁ H ₁₀ O ₃ + H] ⁺ 169.0861, 143.1072, 125.0966 [M − COOH − OH − H] [−] , 123.0811, 97.0654 [M − 2COOH − H] [−] , 57.0343 287.0548 , 258.0511 [M − CO + H] ⁺ , 183.0288, 165.0183, 153.0189 [M − CO − C ₇ H ₆ O + H] ⁺ , 133.0292, 121.0281	96.8	Standard, [46]	CR, CC, C. cassia leaves
32	Quercetin	15.36	C ₁₅ H ₁₀ O ₇	302.0424	−0.98	303.0499 [M + H] ⁺	303.0496 [M + H] ⁺		99.8	[29,35]	CR
33	Quercitrin	15.36	C ₂₁ H ₂₀ O ₁₁	448.1003	−0.58	449.1089 [M + H] ⁺	449.1087 [M + H] ⁺		82.8	Standard	
34	Graveobioside A	15.36	C ₂₆ H ₂₈ O ₁₅	580.1402	−4.46	579.1344 [M − H] [−]	579.1325 [M − H] [−]		85.3		
35	Libertellenone B	15.74	C ₂₀ H ₂₆ O ₄	330.1830	−0.32	331.1903 [M + H] ⁺	331.1902 [M + H] ⁺		75.2		
36	Yucalexin P-17	16.06	C ₁₇ H ₂₀ O ₃	272.1412	0.27	273.1485 [M + H] ⁺	273.1488 [M + H] ⁺		86.6		
37	Azelaic acid	16.24	C ₉ H ₁₆ O ₄	188.1040	0.12	187.0965 [M − H] [−]	187.0966 [M − H] [−]		95.4	[15,47]	CR
38	Kaempferol	16.27	C ₁₅ H ₁₀ O ₆	286.0475	−0.89	287.0550 [M + H] ⁺	287.0548 [M + H] ⁺		99.2	[35]	CR, CC, C. cassia leaves
39	1-(Carboxymethyl) cyclohexane carboxylic acid	16.36	C ₉ H ₁₄ O ₄	186.0884	1.06	185.0808 [M − H] [−]	185.0819 [M − H] [−]		87.2		
40	Kaempferol-3-O- α -L-arabinopyranosyl-7-O- α -L-rhamnopyranoside	16.64	C ₂₆ H ₂₈ O ₁₄	564.1456	−4.12	563.1393 [M − H] [−]	563.1384 [M − H] [−]			[48]	

Table 1. Cont.

NO.	Name	RT	Formula	Calc. MW	Error (ppm)	Theoretical Mass (m/z)	Experimental Mass (m/z)	MS ² (m/z)	Total Score (%) ^a	Ref.	Source ^b
41	2-Methoxy benzaldehyde	16.67	C ₈ H ₈ O ₂	136.0522	−0.16	137.0597 [M + H] ⁺	137.0596 [M + H] ⁺	109.0647, 107.0490 [M − OCH ₂ + H] ⁺ , 93.0698 [M − CO − CH ₃ + H] ⁺ , 81.0697, 79.0512 [M − CO − OCH ₃ + H] ⁺	90.9	[28]	CR, <i>C. cassia</i> leaves
42	Cinnamyl alcohol	17.22	C ₉ H ₁₀ O	134.0726	−0.89	117.0698 [M + H − H ₂ O] ⁺	117.0696 [M + H − H ₂ O] ⁺	117.0696 [M − H ₂ O + H] ⁺ , 91.0540 [M − C ₂ H ₄ O + H] 78.2648 [M − C ₃ H ₅ O + H] ⁺ , 63.4672, 49.4958		standard	CR, CC, <i>C. cassia</i> leaves
43	4-Methylumbelliferyl- α -D-glucopyranoside	17.37	C ₁₆ H ₁₈ O ₈	338.1002	0.21	339.1074 [M + H] ⁺	339.1075 [M + H] ⁺	321.0970 [M − OH + H] ⁺ , 177.0546 [M − C ₆ H ₁₀ O ₅ + H] ⁺ , 145.0284 [M − C ₆ H ₁₀ O ₅ − CH ₃ − OH + H] ⁺ , 127.0389 [M − C ₆ H ₁₀ O ₅ − CH ₃ − OH + H] ⁺ , 97.0280	94.6		
44	(±)-Abscisic acid	17.55	C ₁₅ H ₂₀ O ₄	264.1359	−0.85	265.1484 [M + H] ⁺	265.1481 [M + H] ⁺	247.1332 [M − H ₂ O + H] ⁺ , 229.1216 [M − 2H ₂ O + H] ⁺ , 187.1108 [M − O − CH ₂ − COO + H] ⁺	90.2		
45	<i>trans</i> -Cinnamic acid	18.16	C ₉ H ₈ O ₂	148.0518	−0.60	149.0232 [M + H] ⁺	149.0231 [M + H] ⁺	144.9817 , 131.0493 [M − H ₂ O + H] ⁺ , 121.0282 , 116.9669, 107.0491 , 105.0539 [M − CO + H] ⁺ , 93.0698, 79.0545		Standard [28,30]	CR, CC, <i>C. cassia</i> leaves
46	4-Phenyl-3-buten-2-one	18.31	C ₁₀ H ₁₀ O	146.0730	−1.03	147.0803 [M + H] ⁺	147.0803 [M + H] ⁺	132.0567 [M − CH ₃ + H] ⁺ , 129.0699, 119.0854, 117.0698, 107.0489 [M − CH − CO + H] ⁺ , 91.0541 [M − C ₃ H ₄ O + H] ⁺ , 79.0542	95.3	[32,49]	<i>C. verum</i>
47	3-Tert-butyladipic acid	18.32	C ₁₀ H ₁₈ O ₄	202.1196	−1.36	201.1121 [M − H] [−]	201.1120 [M − H] [−]	183.1021 [M − OH − H] [−] , 156.8982 [M − COO − H] [−] , 139.1124	70.0	[30]	
48	<i>trans</i> -Cinnamaldehyde	18.84	C ₉ H ₈ O	132.0573	−0.19	133.0647 [M + H] ⁺	133.0646 [M + H] ⁺	115.0540 [M − H ₂ O + H] ⁺ , 105.0697 [M − CO + H] ⁺ , 103.0542, 91.0541 [M − CO − CH ₂ + H] ⁺ , 79.0542 [M − CO − C ₂ H ₂ + H] ⁺ , 55.0178 [M − C ₆ H ₆ + H] ⁺	97.9	Standard, [30]	CR, CC
49	2-Methoxycinnamic acid	19.54	C ₁₀ H ₁₀ O ₃	178.0629	−0.51	161.0597 [M + H − H ₂ O] ⁺	161.0596 [M + H − H ₂ O] ⁺	146.0366 , 133.1011 [M − H ₂ O − CO + H] ⁺ , 119.0855 [M − CHO − OCH ₃ + H] ⁺ , 105.0698 [M − COOH − CH + H] ⁺ , 91.0544 [M − CO − CH ₂ − OCH ₃ + H] ⁺		Standard, [30]	CR, CC, <i>C. cassia</i> leaves
50	9S,13R-12-Oxophytodienoic acid	20.08	C ₁₈ H ₂₈ O ₃	292.2037	−0.68	293.2111 [M + H] ⁺	293.2104 [M + H] ⁺	275.2003 [M − H ₂ O + H] ⁺ , 257.1893, 239.1799 [M − C ₄ H ₆ + H] ⁺ , 229.1953, 163.1117, 159.1167, 147.1163 [M − C ₇ H ₁₄ + H] ⁺ , 133.1012, 107.0855, 95.0853, 81.0698 [M − C ₁₂ H ₂₀ O ₃ + H] ⁺ , 69.0699	91.0	[50]	
51	Corchorifatty acid F	20.43	C ₁₈ H ₃₂ O ₅	328.2237	−0.10	327.2166 [M − H] [−]	327.2165 [M − H] [−]	309.2062, 291.1955, 242.9845 [M − C ₅ H ₄ − OH − H] [−] , 239.1283, 229.1435, 221.1171, 211.1313, 185.1173, 183.1374, 171.101 [M − C ₉ H ₁₆ O ₂ − H] [−] , 137.0968, 97.0655, 85.0290 [M − C ₁₃ H ₂₂ O ₄ − H] [−] , 57.0343		[34,51]	

Table 1. Cont.

NO.	Name	RT	Formula	Calc. MW	Error (ppm)	Theoretical Mass (m/z)	Experimental Mass (m/z)	MS ² (m/z)	Total Score (%) ^a	Ref.	Source ^b
52	Deoxyphomalone	20.47	C ₁₃ H ₁₈ O ₄	238.1204	−0.29	239.1277 [M + H] ⁺	239.1275 [M + H] ⁺	221.1171, 205.1192 [M − 2OH + H] ⁺ , 179.0705 [M − C ₂ H ₅ − OCH ₃ + H] ⁺ , 174.0678, 163.0750, 151.0753 [M − C ₂ H ₅ − C ₃ H ₇ O + H] ⁺ , 137.0598 [M − 2OH − 2OCH ₃ − C ₂ H ₄ − C ₃ H ₃ + H] ⁺ , 135.0799, 107.0481 , 95.0861 [M − OH − 2OCH ₃ − C ₂ H ₅ − C ₄ H ₃ O + H] ⁺ , 59.0490	74.4		
53	4-Ethylbenzaldehyde	20.73	C ₉ H ₁₀ O	134.0730	−0.14	135.0804 [M + H] ⁺	135.0803 [M + H] ⁺	120.0567, 107.0490 [M − CO + H] ⁺ , 105.0697 [M − C ₂ H ₆ + H] ⁺ , 103.0542, 79.0542 [M − C ₂ H ₆ − CO + H] ⁺	92	[52]	CR
54	1-Naphthol	21.00	C ₁₀ H ₈ O	144.0573	−0.09	145.0648 [M + H] ⁺	145.0647 [M + H] ⁺	116.0575 [M − C − OH + H] ⁺ , 115.0541, 102.0468 [M − C ₂ H ₂ − OH + H] ⁺ , 91.0539 [M − C ₃ H ₂ − OH + H] ⁺ , 84.9598	89	[53,54]	CR
55	4-Methoxy cinnamaldehyde	21.02	C ₁₀ H ₁₀ O ₂	162.0679	0.04	163.0753 [M + H] ⁺	163.0754 [M + H] ⁺	145.0650, 135.0805 [M − CO + H] ⁺ , 133.0648, 110.0203 [M − C ₃ H ₃ O + H] ⁺ , 107.0491, 105.0699 [M − CO − OCH ₃ + H] ⁺ , 91.0542, 79.0542 [M − C ₃ H ₃ O − OCH ₃ + H] ⁺ , 55.0178	88.4	[46]	CR, CC
56	9,12,13-Trihydroxy-15-octadecenoic acid	21.72	C ₁₈ H ₃₄ O ₅	330.2393	−0.05	329.2322 [M − H] [−]	329.2322 [M − H] [−]	311.2227 [M − H ₂ O − H] [−] , 293.2102 [M − 2H ₂ O − H] [−] , 229.1433, 211.1331, 183.1383, 171.1018, 139.1123, 127.1120, 125.0975, 99.0812, 57.0342	90.0		
57	(−)-Caryophyllene oxide	22.32	C ₁₅ H ₂₄ O	220.1826	−0.53	221.1899 [M + H] ⁺	221.1900 [M + H] ⁺	203.1795, 175.1483 [M − O − 2CH ₂ − C + H] ⁺ , 161.1323 [M − 2CH ₃ − CO − CH + H] ⁺ , 147.1169 [M − 2CH ₃ − CO − CH − CH ₂ + H] ⁺ , 133.1010, 119.0855, 95.0855	92.9	[55]	CR, CC, C. cassia leaves
58	4-Methoxychalcone	28.61	C ₁₆ H ₁₄ O ₂	238.0992	0.66	239.1066 [M + H] ⁺	239.1073 [M + H] ⁺	221.0961, 193.1012, 178.0875, 161.0595 [M − C ₆ H ₆ + H] ⁺ , 133.0647 [M − C ₇ H ₆ O + H] ⁺ , 115.054, 105.0333 [M − C ₆ H ₆ − C ₂ H − OCH ₃ + H] ⁺	86.7	[56]	C. cassia

^a indicated that the comprehensive score of molecular formula, molecular structure and MS² fragment ions matching with the mzCloud database. ^b indicated that this compound has been isolated or identified from a certain plant. Bold is their MS² fragment ion that matched the standard. Bold and italicize is the diagnostic ion for each compound.

Compound **48** obtained a precursor ionic peak at m/z 133.0645 in the ESI (+) mode; its molecular formula of the compound was C_9H_8O and it had a molecular weight of 132.0572 based on the elemental composition analysis. The matching fragments were mainly m/z 115.0540 $[M - H_2O + H]^+$, m/z 105.0696 $[M - CO + H]^+$, m/z 91.0540 $[M - CO - CH_2 + H]^+$, m/z 79.0542 $[M - CO - C_2H_2 + H]^+$ and m/z 55.0177 $[M - C_6H_6 + H]^+$ (Table 1), which was consistent with the cleavage fragment of *trans*-cinnamaldehyde in the literature and database: the compound was, therefore, presumed to be *trans*-cinnamaldehyde [57]. The MS² spectrum of compound **48** is shown in Figure S6, and the possible cleavage process of the positive ions was shown in Figure 2.

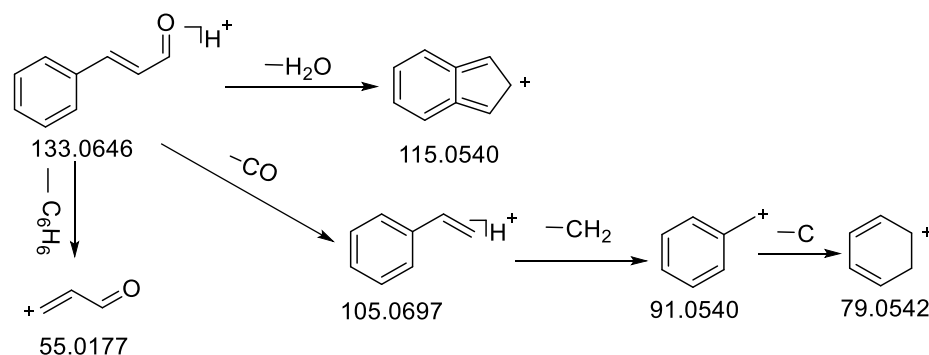


Figure 2. Fragmentation pathway of *trans*-cinnamaldehyde in positive ion mode.

2.2.2. Identification of Flavonoids

The RDA cleavage of the C-ring was the main cleavage of flavonoids, resulting in fragment ions and the loss of a series of neutral small molecules such as H_2O , CO_2 , and CO by energy collisions under certain mass spectrometric conditions [25,58]. Flavonoid oxyglycosides generally lost sugar first, and then cleaved according to the cracking law of flavonoid skeleton structure [26,59]. Combined with the mass fragments information in the literature and standards, the ionic fragments at m/z 291/289, 303/301, 287/285 were selected, respectively, as the diagnostic ion for epicatechin-type, quercetin-type, and kaempferol-type [23]. The cracking of flavonoids and dihydroflavones was very similar, for example, epicatechin (**11**) and quercetin (**32**) demonstrated the cracking laws of epicatechin-type and quercetin-type, as shown in Figures 3 and 4, the MS² spectrum of epicatechin (**11**) is shown in Figure S7.

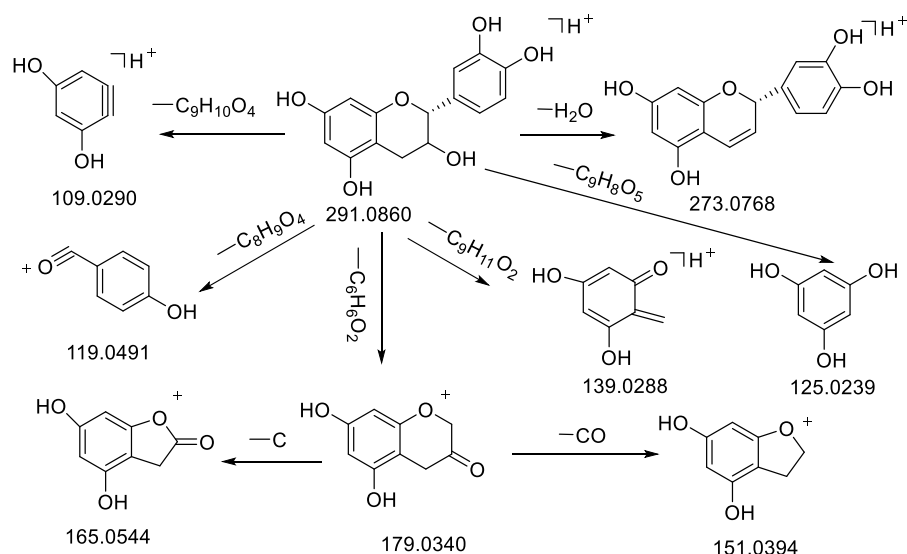


Figure 3. Fragmentation pathway of epicatechin in positive ion mode.

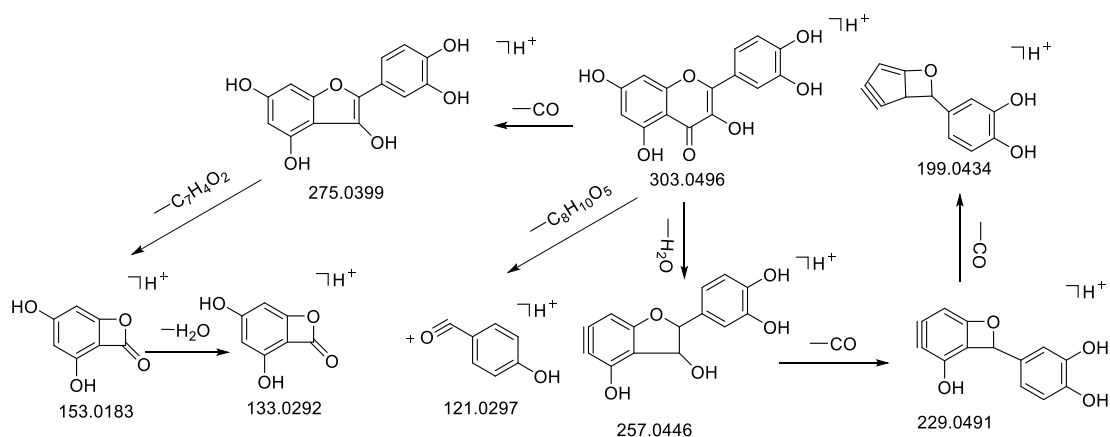


Figure 4. Fragmentation pathway of quercetin in positive ion mode.

Compound **11** had the molecular formula of $C_{15}H_{14}O_6$ which resulted from a precursor ion at m/z 291.0860 $[M + H]^+$, and preeminently from an H_2O loss at the fragment peak m/z 273.0768 $[M - H_2O + H]^+$ [26]. This was caused, first, by the loss of $C_6H_6O_2$ obtaining m/z 179.0340 $[M - C_6H_6O_2 + H]^+$, then by the loss of CH_2 and CO , obtaining m/z 165.0544 $[M - C_6H_6O_2 - CH_2 + H]^+$ and m/z 153.0376 $[M - C_6H_6O_2 - CO + H]^+$. Moreover, losses of $C_9H_8O_3$, $C_8H_9O_4$, $C_9H_{11}O_2$ and $C_9H_{10}O_4$ formed m/z 125.0239 $[M - C_9H_8O_3 + H]^+$, m/z 119.0491 $[M - C_8H_9O_4 + H]^+$, m/z 139.0388 $[M - C_9H_{11}O_2 + H]^+$ and m/z 109.0290 $[M - C_9H_{10}O_4 + H]^+$ (Table 1, Figure 3), This was consistent with the cleavage fragment of epicatechin in the literature and standards; accordingly, the compound was presumed to be epicatechin [59].

Compound **32** had the molecular formula $C_{15}H_{10}O_7$ which resulted from a precursor ion at m/z 303.0496 $[M + H]^+$ in the ESI (+) mode; this was primarily caused by losses of H_2O and CO and formed m/z 257.0446 $[M - CO - H_2O + H]^+$; $2CO$ loss then occurred and m/z 229.0491 $[M - 2CO - H_2O + H]^+$, and m/z 199.0434 $[M - 3CO - H_2O + H]^+$ were obtained. In contrast, a loss of $C_7H_4O_2$ formed m/z 153.0183 $[M - CO - C_7H_6O_2 + H]^+$, followed by a loss of H_2O to form m/z 133.0292 $[M - CO - C_7H_4O_2 - H_2O + H]^+$ (Table 1, Figure 4). This was consistent with the cleavage fragment of quercetin in the literature [59] and standards, so the compound was presumed to be quercetin.

2.2.3. Identification of Coumarins

The main cleavage of coumarins included the losses of OH , CH_3 and CO_2 from characteristic substituents and the continuous neutral loss of CO from the pyran ring [58,60]. The fragmentation rule for the coumarin glycosides was similar to that for coumarins, except for the initial losses of sugar moieties.

As an example, compound **31** obtained a quasi-ionic peak at m/z 147.0439 $[M + H]^+$ in ESI (+) mode, and the molecular formula for this compound was $C_9H_6O_2$. The matching fragments were mainly m/z 103.0541 $[M + H - CO_2]^+$ and m/z 91.0540 $[M + H - 2CO]^+$ (Table 1). This was consistent with the cleavage fragment of coumarin in the literature [61,62] and standard, so **31** was presumed to be coumarin. The MS^2 spectrum of compound **31** was shown in Figure S8, and the possible cleavage process of the positive ions is shown in Figure 5.

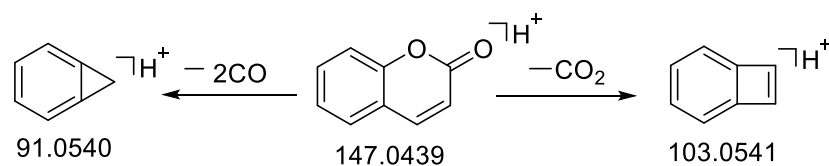


Figure 5. Fragmentation pathway of coumarin in positive ion mode.

Identification information of other compounds were detailed in Sections S1–S7 of Supplementary Materials.

2.3. Statistical Analysis

The MS data from different sources of CR and CC were imported into Compound Discoverer 3.2 qualitative analysis software for normalization and export, with a total of 1460 positive and negative ion fragments. The processed data were imported into SICMA 14.1 software for statistical analysis, resulting in the designation of 37 discrepant compounds. Analysis of variance was performed on the discrepant compounds using GraphPad Prism 7.0 software, resulting in 26 statistically significant ($p < 0.05$) discrepant compounds.

2.3.1. Principal Component Analysis (PCA)

PCA analysis can clearly explain the correlation between a large number of variables and a small number of principal components with less data loss; this can effectively reduce the dimensionality of the multidimensional raw data. The results showed that the CR and CC samples could be clearly separated and classified into one category, indicating that there were differences in the chemical compositions of CR and CC. When statistical analysis was used, the QC samples should be included to evaluate the instrument stability. The results of the PCA analysis are shown in Figure S9.

2.3.2. Orthogonal Partial Least Squares-Discriminant Analysis (OPLS-DA)

The difference in the chemical compositions of CR and CC was further studied using supervised OPLS-DA; the score diagram was shown in Figure S10. The results indicated that CR and CC can be clearly separated, which was consistent with the PCA results. The model fitting was also validated by setting the number of tests to 200. The R^2 and Q^2 points on the left of the data were lower than the original values on the right, and the regression line at the Q^2 intersected the vertical axis below the original point with a negative nodal increment. The results of the model validation were $R^2Y = 0.999$ and $Q^2 = 0.952$ (R^2 in the validation results represented the matching of the model. The closer R^2 to 1, the more complete the model was in describing the data; the closer Q^2 to 1, the higher the predictive ability of the model) (Figure S11). Model evaluation results indicated that the model had robustness and no over-fitting. The commonly used variable importance for the project (VIP) was used to estimate for quality difference markers between groups. Variables with a $VIP > 1$ was generally considered to be meaningful to the model, the greater the VIP value was, the greater the contribution of the variable. Therefore, a $VIP > 1$ was selected to analyze the overall variability of CR and CC to find differential markers (Figure S12). A total of 627 characteristic peaks was determined for the differential components ($VIP > 1$) that contributed significantly to the classification of CR and CC (Table S2). A total of 37 differential compounds with $VIP > 1$ was identified based on the analysis of compound retention times, accurate relative molecular masses, and cleavage information. Information on compounds with $VIP > 1$ were shown in Table S2. The peak areas of these 37 compounds were subjected to t -tests using GraphPad Prism7.0 software, resulting in 26 chemical components with $VIP > 1$ and $p < 0.05$, including compounds 1–3, 5, 8, 16, 17, 19, 24, 26, 27, 31–36, 38, 40–42, 45, 46, 48, 53 and 58, These comprised two organic acids, six phenolic acids, seven phenylpropanoids, eight flavonoids, two terpenoids and one coumarin. According to the peak areas and secondary fragment information, of the 26 significantly different compounds, 6 (19, 32, 33, 38, 41 and 53) were specific to CR, and 3 (8, 26, and 36) were specific to CC.

2.3.3. Semi-Quantitative Analysis of CR and CC

A semi-quantitative analysis was further carried out to compare the intensity trends of CR and CC by calculating the relative peak areas of 26 compounds in 16 samples. The box-plots could visually observe the content changes between chemical compositions. The peak

areas data for the 26 compounds in CR and CC were exported, and the boxplots produced by GraphPad Prism 7.0 software were further used to compare the relative content of the compounds in CR and CC, as shown in Figure 6.

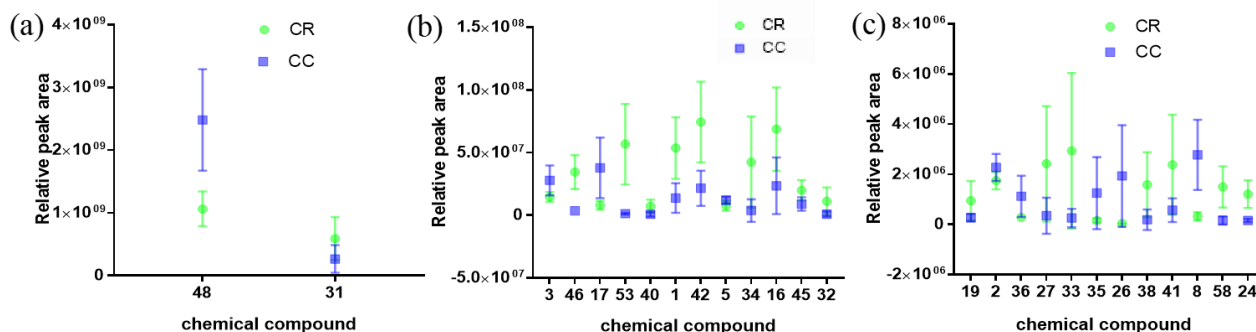


Figure 6. Box plots of the relative intensities of CR and CC: (a) compounds 48 and 31 with peak areas of 3.52×10^7 – 3.17×10^9 ; (b) compounds 3, 46, 17, 53, 40, 1, 42, 5, 34, 16, 45 and 32 with peak areas of 4.80×10^5 – 1.48×10^8 ; and (c) compounds 19, 2, 36, 27, 33, 35, 26, 38, 41, 8, 58 and 24 with peak areas of 3.15×10^4 – 6.15×10^6 .

The results (Figure 6) showed that the peak areas of compounds 1, 16, 19, 24, 27, 31, 32, 33, 34, 38, 40, 41, 42, 45, 46, 53 and 58 in CR were higher than those in CC. Among these compounds, compounds 19, 27, 32, 33, 38, 40 and 41 were flavonoids and flavonoid glycosides; 16, 41, 42, 45, 46, 53 and 58 were phenylpropanoids; 1 and 24 were organic acids; 31 was coumarin and 34 was lignan glycoside. The peak areas of compounds 2, 3, 5, 8, 17, 26, 35, 36 and 48 in CC were higher than those in CR. Among them, *trans*-cinnamaldehyde (48) was the major active components in both CR and CC. Compound 26 was flavonoid glycoside; 2, 3, 8 and 17 were organic acids; 35 and 36 were terpenoids and 5 was catechol.

Accordingly, the peak areas of flavonoids and flavonoid glycosides, and phenylpropanoids except *trans*-cinnamaldehyde in CR were higher than in CC, and the peak areas of terpenoids and organic acids in CC were higher than in CR.

2.4. Method Validation

The relative standard deviations (RSDs) for the precision, stability, and repeatability investigations into of coumarin, cinnamyl alcohol, cinnamic acid, dimethoxy cinnamic acid and cinnamaldehyde were all <5% (Table 2), indicating that the method had good precision, repeatability, and recovery. Additionally, a recovery range of 97–101% (RSD < 4%) indicated its high recovery and reliability (Table S3).

Table 2. Linear-regression data, precision, stability, and repeatability of five standard compounds.

No.	Name	Linear	r	Linear Range (µg/mL)	Precision (RSD) n = 6	Stability (RSD) n = 6	Repeatability (RSD) n = 6	Average Recovery (%)	Recovery RSD (%)
31	Coumarin	Y = 1118.3X – 1.9591	0.9998	1.0331–1033.31	0.43%	0.83%	2.48%	100.09%	2.42%
42	Cinnamyl Alcohol	Y = 1377.2X – 0.0481	0.9997	0.0187–3.7300	2.30%	1.17%	2.81%	98.07%	2.77%
45	<i>trans</i> -Cinnamic acid	Y = 3219.7X – 1.3026	0.9999	0.6667–6.6670	0.47%	0.65%	1.60%	95.11%	2.09%
48	2-Methoxy cinnamic acid	Y = 12307X – 0.0527	0.9997	0.0133–2.6660	0.70%	0.74%	1.56%	98.30%	2.23%
49	<i>trans</i> -Cinnamaldehyde	Y = 449.01X – 5.4428	0.9995	108.30–2800	2.48%	3.43%	2.67%	97.36%	3.43%

2.5. Quantitative Determination of the Major Constituents in CR and CC Using HPLC

The established HPLC analysis method was subsequently used to determine the representative components in eight batches of CR and CC products. In the case of quantitative analysis, all the samples (eight batches of CR and CC) were extracted three times and analyzed by HPLC. The RSD value of the concentrations of these five standards were less than 5%. The HPLC chromatograms were shown in the Figure S13. The contents of the five compounds are summarized in Table 3, based on their respective calibration curves. The results showed that there were significant differences in the composition content of CR and CC. Among them, the content of *trans*-cinnamaldehyde in CC was about twice that in CR, and the content of *trans*-cinnamic acid in CC was similar to that in CR; the contents of coumarin, cinnamyl alcohol and 2-methoxycinnamic acid in CC were significantly higher than those in CR. We, therefore, believe that these five components play a key role in the different efficacies of CR and CC.

Table 3. The contents of 5 analytes in 8 batches of CR and CC.

Sample	Coumarin (mg/g)	Cinnamyl Alcohol (mg/g)	<i>trans</i> -Cinnamic Acid (mg/g)	2-Methoxycinnamic Acid (mg/g)	<i>trans</i> -Cinnamaldehyde (mg/g)
CR-1	1.2038	0.0381	1.2205	0.0180	26.9798
CR-2	0.8544	0.0602	0.4867	0.0055	24.3722
CR-3	0.4209	0.1431	0.2674	0.0021	17.0832
CR-4	0.7392	0.0770	0.4862	0.0057	29.9873
CR-5	0.4531	0.0479	0.5113	0.0017	19.6756
CR-6	0.4834	0.0839	0.5245	0.0017	16.1460
CR-7	0.5107	0.0849	0.3960	0.0016	16.4895
CR-8	0.3563	0.1241	0.2769	0.0017	13.3894
CC-1	0.7534	0.0141	0.4164	0.0032	49.7582
CC-2	0.4307	0.0440	0.3474	0.0006	64.4378
CC-3	0.1880	0.0052	0.2370	0.0005	42.3951
CC-4	0.1611	0.0130	0.2914	0.0003	52.0785
CC-5	0.2030	0.0163	0.0811	0.0003	36.8182
CC-6	0.5814	0.0161	0.3301	0.0011	40.5779
CC-7	0.3655	0.0177	0.2932	0.0012	52.9302
CC-8	0.3851	0.0212	0.3169	0.0014	54.7701

2.6. Cluster Analysis

The original data of our compound content was imported into Lianchuan Biotechnology's advanced heat map statistics software, and the original data was normalized by Z-score to obtain the result (Figure S14). As our statistics result indicated, CR and CC were each clustered into one group. Five compounds were screened out and could be used as chemical markers for distinguishing CR and CC; Among the five, two markers including *trans*-cinnamaldehyde and cinnamyl alcohol (VIP value is greater than the other three compounds) made greater contributions to sample grouping than the other three ones.

2.7. Molecular Docking

The different screened constituents were docked to PGC1 α (PDB ID: 1XB7), SIRT3 (PDB ID: 4BN4) and AMPK (PDB ID: 4CFF). CDOCKER_INTERACTION_ENERGY \leq -5.0 kJ/mol was used to produce a better binding ability for the compounds and proteins. The results were shown in Table S4 and Figure 7.

The results showed that compounds **40**, **34**, **17**, **26** and **27** had the highest binding energy with Glycosylated Hemoglobin, Type A1C (HbA1c); compounds **1**, **32**, **16** and **19** had the highest binding energy with peroxisome proliferator-activated receptor-gamma coactivator-1alpha (PGC1 α); compounds **24**, **2**, **45**, **42** and **3** had the highest binding energy with silent information regulator protein 3 (SIRT3); and compounds **40**, **33**, **34**, **27** and **32** had the highest binding energy with AMP-activated protein kinase (AMPK). Among these

compounds, only 2, 3, 17, 26 had a higher content in CC. These results demonstrated that the special and high-concentration components in CR showed high docking scores of affinities with targets such as HbA1c and the proteins in the AMPK–PGC1–SIRT3 signaling pathway, suggesting the greater potentials for CR in treating DPN than for CC. The compounds with high protein binding energy were phenylpropanoid (1, 16, 42, 45) and flavonoids (19, 26, 27, 40).

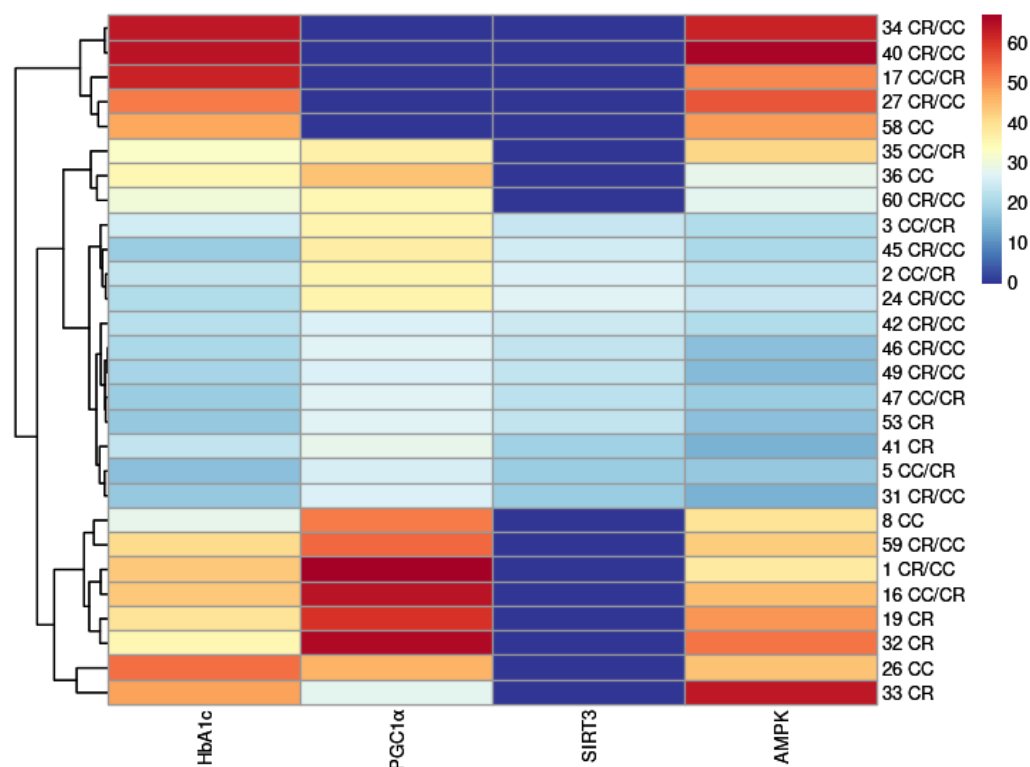


Figure 7. Heatmap of molecular docking.

3. Materials and Methods

3.1. Materials and Reagents

The following were used: the UPLC-Oribtrap-Exploris-120-MS liquid chromatography-mass spectrometry system (Thermo Scientific, Waltham, MA, USA); a KQ-500B CNC Ultrasonic Cleaner (Kunshan Ultrasonic Instrument Co., Ltd., Kunshan, China); methanol, acetonitrile, formic acid (chromatographic grade, Fisher, Waltham, MA, USA); ultra-pure water was freshly prepared using a Milli-Q system (Millipore, Milford, MA, USA); a high speed refrigerated centrifuge (Thermo Fisher, Karlsruhe, Germany); Watsons purified water. *trans*-Cinnamaldehyde (104-55-2), *trans*-cinnamic acid (621-82-9), cinnamyl alcohol (104-54-1), coumarin (91-64-5) and dimethoxy cinnamic acid (6099-03-2) were purchased from Chengdu purechem-standard co. LTD; epicatechin (490-46-0), taxifolin (480-18-3) and quercetin (522-12-3) were purchased from Shanghai yuanye Bio-Technology Co., Ltd.; and the purities of all the standards were greater than 98%. The eight batches of Cinnamomi ramulus (CR) and Cinnamomi cortex (CC) that were respectively the dried twigs and bark of *Cinnamomum cassia* Presl, were collected from different locations (Guangxi, Guangdong and Sichuan) at different harvest times (2019, 2020 and 2021), and stored in engineering technology research center for the comprehensive development and utilization of authentic medicinal materials in Henan province, as shown in Table S5.

3.2. Preparation of Sample Solutions

Each CR and CC sample was weighed (1 g) accurately and extracted under reflux with 50 mL ultrapure water for 2 h. They were left to reach room temperature; water was then added to compensate for the weight loss of the extraction solution. A volume of 1 mL of the extraction solution was diluted with methanol to 2 mL; this was filtered through a 0.22 µm nylon filter membrane and centrifuged at 12,000 rpm for 15 min for UPLC-MS analysis. A volume of 1 mL of the extraction solution was directly filtered and centrifuged for HPLC quantitative analysis. Mixed standard solutions (*trans*-cinnamaldehyde, *trans*-cinnamic acid, epicatechin, 2-methoxycinnamic acid and quercitrin) were used as QC samples.

3.3. Preparation of Reference Solutions

An appropriate amount of the reference materials of coumarin, cinnamyl alcohol, cinnamic acid, 2-methoxycinnamic acid and cinnamaldehyde were measured and weighed precisely; methanol was added to dissolve them, and 1.0331, 1.8667, 0.6667, 1.1333 and 3.4 mg/L, respectively, were prepared for standby.

3.4. Chromatography and Mass Spectrometry Conditions

3.4.1. UPLC Method for Qualitative Analysis

Qualitative analysis was performed on UPLC-Orbitrap-Exploris-120-MS and the preferred column was achieved on A HYPERSILGOLD Vanquish C18 (2.1 mm × 100 mm, 1.9 µm) for chromatographic separation. The mobile phase consisted of acetonitrile (A) and 0.1% aqueous formic acid (B), with a flow rate of 0.3 mL/min, and the gradient elution condition was set as follows: 0~4 min, 5~8% A; 4~10 min, 8~16% A; 10~15 min, 16% A; 15~22 min, 16~30% A; 22~25 min, 30% A; 25~32 min, 30~40% A; 32~35 min, 50% A; 35~40 min, 50~90% A. The injection volume was 1 µL and the column temperature was 25 °C.

3.4.2. UPLC-MS Method for Qualitative Analysis

MS data was acquired in fast chromatography MS² mode, the mass spectrometer parameters were set as follows: The ESI was used in negative ion mode (ESI⁻) and in positive ion mode (ESI⁺). The following settings were used: the spray voltage was 2.5 kV(−) and 3.5 kV(+); the UHPLC-MS/MS mode was applied with an Orbitrap resolution of 120,000 for full-MS and 15,000 for dd-MS²; the isolation window (*m/z*) was 2; the RF Lens% was 70; the sheath gas pressure was 45 Arb; the auxiliary gas pressure was 15 Arb; the sweep gas pressure was 0 Arb; the capillary temperature was 320 °C; vaporizer temperature was 350 °C; the scanning range was *m/z* 80~800; the stepped normalized collision energies (NCE) were 15, 30 and 45 eV.

3.4.3. HPLC Method for Quantitative Analysis

The major active components including coumarin, cinnamyl alcohol, *trans*-cinnamic acid, 2-methoxycinnamic acid and *trans*-cinnamaldehyde were used for quantitative analysis.

Quantitative analysis was performed on a Waters HPLC E2695 and the preferred column was achieved on a Waters C18 (4.6 mm × 250 mm, 5 µm) for the chromatographic separation. The mobile phase was consisted of acetonitrile (A) and 0.1% aqueous formic acid (B), with a flow rate of 1 mL/min, and the gradient elution condition was set as follows: 0~13 min, 5~15% A; 13~20 min, 15~26% A; 20~25 min, 26% A; 25~28 min, 26~30% A; 28~38 min, 30%~40% A; 38~48 min, 40~60% A; 48~52 min, 60%~95% A; 52~57 min, 95% A. The injection volume was 20 µL, and column temperature was 30 °C.

To evaluate linearity, a series of standard solutions with appropriate concentrations were obtained by diluting standard compounds with methanol. The calibration curves were drawn with the quality of the reference substance as the abscissa (X) and the peak area as the ordinate (Y), they showed a good linear relationship ($r \geq 0.999$) within the test ranges. The same sample solutions of CR and CC were continuously injected to verify the precision of the instrument. The same sample solutions were injected, separately, 0, 2, 4,

8, 12, and 24 h separately to check the stability of the test solution. Six sample solutions were prepared independently to verify the repeatability of the method. The accuracy of the method was evaluated by a recovery test. Recovery (%) = $\{[\text{Found} - (\text{Original sample} + \text{Add})]/\text{Add}\} * 100$.

3.4.4. LC-MS Data Processing and Statistics

The UPLC-Orbitrap-Exploris-120-MS data were acquired by the Trancefinder 5.1 software; the UHPLC-MS/MS mode was applied with an Orbitrap resolution of 120,000 for full-MS and 15,000 for dd-MS². The data was then analyzed using the Xcalibur3.0 software. Each raw data processed using Compound Discoverer 3.2 qualitative analysis software following a specific workflow (Figure S15). The screening steps of the target compound were: All ions presenting a signal over 5 times the background noise and a peak intensity over 10⁵ were taken into account to create the extracted ion chromatogram (EIC). MS and MS² spectra were then used to identify ions by searching the mzCloud, mzValut, Chemspider and mass Lists databases. Then select the matching compounds with a tolerance of 5 ppm and more than 60% of the database matching degree as our preliminary identified compound. Finally, the compounds were reconfirmed by combined with the parent ion and the MS² fragment ions extracted from their original data with those in the relevant literature. Additionally, the compounds were all rechecked by searching literature materials to exclude the non-natural products. The peak area of fragment ions was statistically analyzed to determine the statistically significant difference components, and then the marker compounds were clustered for the purpose of distinguishing CR and CC.

To evaluate relationships on the basis of similarities or differences between groups of multivariate data, multivariate analyses (PCA and OPLS-DA) were performed using SIMCA 14.1. PCA results were displayed in the form of score plots. OPLS-DA was conducted using class information as the Y-variable; the results were shown in the form of score plots. The contribution of variables to the analysis was explained using variable importance in projection (VIP) scores. VIP scores are a weighted sum of squares of PLS weights, with scores larger than 1 indicating variables are important to the mode. T-tests were performed for compounds with VIP > 1: compounds with *p* value of <0.05 were considered significantly differentiated compounds.

3.4.5. Molecular Docking

We used Discovery Studio to predict the docking of small molecule compounds with key proteins. The 3D structure of the compound constructed by ChemOffice software was saved in *.mol2 format, and its energy was minimized. The 3D structure of the target protein was downloaded from the PDB data (<https://www.rcsb.org/>), accessed on 24 November 2022, and Discovery Studio 2020 software was used to perform operations such as water removal and hydrogenation on the protein and generate an effective single 3D conformation by minimizing the energy.

4. Conclusions

In this study, chemical compounds in CR and CC were analyzed and identified using UPLC-Orbitrap-Exploris-120-MS/MS: a total of 58 chemical components were identified. Unsupervised PCA and supervised OPLS-DA were used to assess the differences between CR and CC, and GraphPad Prism 7.0 was used to perform *t*-tests on the differential components. A total of 26 statistically significant differential compounds were obtained, in which the peak areas of flavonoids (19, 27, 32, 33, 38, 40 and 41) and phenylpropanoids (16, 41, 42, 45, 46, 53 and 58) except cinnamaldehyde in CR were higher than in CC, and the peak areas of terpenoids (35 and 36) and organic acids (2, 3, 8 and 17) in CC were higher than in CR. Additionally, HPLC was used to determine the concentrations and differentiating capacities of coumarin, cinnamyl alcohol, cinnamic acid, 2-methoxycinnamic acid and cinnamaldehyde, which were the major active ingredients in both CR and CC. The results

showed that the content of cinnamaldehyde in CC was about twice that in CR, the content of cinnamic acid in CC was similar to that in CR, and the content of coumarin, cinnamyl alcohol and 2-methoxycinnamic acid in CR were significantly higher than that in CC. These five major components could be used as markers for successfully distinguishing CR and CC [63]. Compared to the reported method in the literature, the quantitative method was simpler, and demonstrated good stability and reproducibility. In addition, the different screened constituents were docked to HbA1c, PGC1 α , SIRT3 and AMPK, and the results showed that the special and high-concentration components in CR showed high docking scores of affinities with targets such as HbA1c or proteins in the AMPK–PGC1–SIRT3 signaling pathway, suggesting the greater potentials of CR in treating DPN than of CC. Furthermore, the compounds with higher protein binding energy were phenylpropanoid (1, 16, 42, 45) and flavonoids (19, 26, 27, 40), from which it be inferred that flavonoids and phenylpropanoids might be an important material basis for the differential efficacies of CR and CC. The above results provide comparative information on the chemical profiles of CR and CC, as well as the groundwork for exploring the effective substances in each.

This is the first time that the compositional differences in the aqueous extracts of CR and CC by LC-MS have been analyzed, which directly reflects the material basis for their different functions under the usage of decoction in clinical practices. The high-content flavonoids and phenylpropanoids in CR may be the key material basis for dispersing wind and cold medicines, and terpenoids and organic acids may be the main active constituents for interior-warming medicines. In previous studies, flavonoids such as quercetin decreased blood glucose levels [64], phenylpropanoids inhibited platelet aggregation [65], and coumarin had suppressive effects on neuropathic cold allodynia in rats [66]. A further investigation of these CR differential substances may make it possible to find effective drugs for treating DPN. The previous studies were mostly focused on *trans*-cinnamaldehyde, while the CR and CC differential components would be easily acquired, combined with modern separation technology, and are worthy of further modern pharmacological research.

Supplementary Materials: The following supporting information can be downloaded at: <https://www.mdpi.com/article/10.3390/molecules28052015/s1>, Figure S1: Typical total ion chromatograms (TIC) of CR (A) and CC (B) in both positive and negative ion modes; Figure S2: Mass spectra and structural formulas of all detected compounds; Figure S3: Identified compound structures; Figure S4: Extracted ion chromatograms (EIC) of 8 standards; Figures S5–S8: The MS² spectra of *trans*-cinnamic acid, *trans*-cinnamaldehyde, epicatechin and coumarin. Figure S9: 2D PCA score scatter plot for CR CC and QC after eliminating outliers; Figure S10: 2D OPLS-DA score scatter plot for CR and CC; Figure S11: Validate model of OPLS-DA. Figure S12: Variable importance of projection (VIP) plot of the OPLS-DA. Figure S13: HPLC chromatograms for quantitative analyses. Figure S14: Dendrograms of hierarchical cluster analysis (HCA) for CR and CC.; Figure S15: The workflow of compound screening with Compound Discoverer 3.2. Table S1: Optimization of the LC-MS conditions; Table S2: Compound information with VIP > 1; Table S3: Results of the recovery test; Table S4: Molecular docking fraction; Table S5: Information on CR and CC. Sections S1–S7: Identification of other constituents of CR and CC. References [67–73] have been cited Supplementary Materials.

Author Contributions: L.-P.D. and Z.-M.W. were responsible for the management. P.W. and J.C. carried out the experiments and data analysis. S.-X.W. and J.W. processed extracted the medicinal materials. P.W., J.C. and H.G. contributed to writing and revising the manuscript. L.-P.D. and E.-P.X. revised the writing of the manuscript. All authors have read and agreed to the published version of the manuscript.

Funding: This work was partially supported by the Key Research Project on Traditional Chinese Medicine Culture and Management of Henan (No. TCM2021013), the Major Increase or Decrease Branch Program of Central level (No. 2060302-1904-24), the National Natural Science Foundation of China (No. 82104035), the Scientific and Technological Innovation Teams of Colleges and Universities in Henan Province (No. 23IRTSTHN028), and the Provincial Key Technologies R&D Program of Henan Province (No. 221100310400).

Institutional Review Board Statement: Not applicable.

Informed Consent Statement: Not applicable.

Data Availability Statement: Data is contained within the article or Supplementary Materials.

Conflicts of Interest: The authors declare no conflict of interest.

References

1. Liu, J.; Zhang, Q.; Li, R.L.; Wei, S.J.; Huang, C.Y.; Gao, Y.X.; Pu, X.F. The traditional uses, phytochemistry, pharmacology and toxicology of *Cinnamomi ramulus*: A review. *J. Pharm. Pharmacol.* **2020**, *72*, 319–342. [[CrossRef](#)]
2. Xiang, H.J.; Zhang, L.S.; Song, J.N.; Fan, B.; Nie, Y.L.; Bai, D.; Lei, H.M. The profiling and identification of the absorbed constituents and metabolites of Guizhi decoction in rat plasma and urine by rapid resolution liquid chromatography combined with quadrupole-time-of-flight mass spectrometry. *Int. J. Mol. Sci.* **2016**, *17*, 1409. [[CrossRef](#)] [[PubMed](#)]
3. Liu, L.; Chu, X.Q.; Tian, C.L.; Xia, M.Q.; Zhang, L.; Jiang, J.Q.; Gui, S.Y. Chemo profiling and simultaneous analysis of different combinations of *Sinomenii caulis* and *Ramulus cinnamomi* using UHPLC-Q-TOF-MS, GC-MS and HPLC methods. *J. Chromatogr. Sci.* **2021**, *59*, 606–661. [[CrossRef](#)] [[PubMed](#)]
4. Wang, D.; Wu, X.M.; Zhang, D.D.; Zhu, B.R.; Wang, S.C.; Wang, C.X.; Jia, Q.; Li, Y.M. Study on chemical constituents of *Cinnamomi ramulus*. *J. Chin. Mat. Med.* **2020**, *45*, 124–132.
5. Wu, X.X.; He, J.; Xu, H.R.; Bi, K.S.; Li, Q. Quality assessment of *Cinnamomi ramulus* by the simultaneous analysis of multiple active components using high-performance thin-layer chromatography and high-performance liquid chromatography. *J. Sep. Sci.* **2014**, *37*, 2490–2498. [[CrossRef](#)] [[PubMed](#)]
6. Gong, Z.; Gong, L.; Hu, L.L.; Han, J.; Gong, Y.Y.; Xing, Y. Comparative Study on volatile oil components of *Rimulus cinnamon* and *Cinnamon*. *J. Liaoning Tradit. Chin. Med. Mag.* **2014**, *41*, 2199–2201.
7. Chen, P.Y.; Yu, J.W.; Lu, F.L.; Lin, M.C.; Cheng, H.F. Differentiating parts of *Cinnamomum cassia* using LC-QTOF-MS in conjunction with principal component analysis. *Biomed. Chromatogr.* **2016**, *30*, 1449–1457. [[CrossRef](#)]
8. Guo, Z.L.; Zhu, P.X.; He, X.A.; Yan, T.H.; Liang, X.R. Components identification and isomers differentiation in pigeon pea (*Cajanus cajan* L.) leaves by LC-MS. *J. Sep. Sci.* **2021**, *44*, 2510–2523. [[CrossRef](#)]
9. Gao, X.; Sun, W.J.; Fu, Q.; Niu, X.F. Ultra-performance liquid chromatography coupled with electrospray ionization/quadrupole time-of-flight mass spectrometry for the rapid analysis of constituents in the traditional Chinese medical formula Danggui San. *J. Sep. Sci.* **2014**, *37*, 53–60. [[CrossRef](#)]
10. Li, J.F.; Chen, W.J.; Wang, Y.H.; Yin, H. An LC-MS/MS method for simultaneous quantification of 11 components of Xian-Xiong-Gu-Kang in the plasma of osteoarthritic rats and pharmacokinetic analysis. *J. Sep. Sci.* **2021**, *44*, 3386–3397. [[CrossRef](#)]
11. Lei, H.B.; Zhang, Y.H.; Ye, J.; Cheng, T.F.; Liang, Y.L.; Zu, X.P.; Zhang, W.D. A comprehensive quality evaluation of Fuzi and its processed product through integration of UPLC-QTOF/MS combined MS/MS-based mass spectral molecular networking with multivariate statistical analysis and HPLC-MS/MS. *J. Ethnopharmacol.* **2021**, *266*, 113455. [[CrossRef](#)] [[PubMed](#)]
12. Zheng, Y.Y.; Zeng, X.; Peng, W.; Wu, Z.; Su, W.W. Characterisation and classification of *Citri Reticulatae Pericarpium* varieties based on UHPLC-Q-TOF-MS/MS combined with multivariate statistical analyses. *Phytochem. Anal.* **2019**, *30*, 278–291. [[CrossRef](#)] [[PubMed](#)]
13. Wang, G.Y.; Shang, J.; Wu, Y.; Ding, G.; Xiao, W. Rapid characterization of the major chemical constituents from *Polygoni multiflori caulis* by liquid chromatography tandem mass spectrometry and comparative analysis with *Polygoni multiflori radix*. *J. Sep. Sci.* **2017**, *40*, 2107–2116. [[CrossRef](#)] [[PubMed](#)]
14. Zeng, L.S.; OuYang, C.X. Effect of integrated traditional Chinese and western medicine on diabetic peripheral neuropathy and its influence on serum levels of homocysteine and cystatin-C. *Chin. Mod. Med.* **2019**, *26*, 151–153,156.
15. Liu, J.; Zhang, Q.; Li, R.L.; Wei, S.J.; Gao, Y.X.; Ai, L.; Wu, C.J.; Pu, X.F. Anti-proliferation and anti-migration effects of an aqueous extract of *Cinnamomi ramulus* on MH7A rheumatoid arthritis-derived fibroblast-like synoviocytes through induction of apoptosis, cell arrest and suppression of matrix metalloproteinase. *Pharm. Biol.* **2020**, *58*, 863–877. [[CrossRef](#)]
16. Han, Y.; Jung, H.W.; Bae, H.S.; Kang, J.S.; Park, Y.K. The extract of *Cinnamomum cassia* twigs inhibits adipocyte differentiation via activation of the insulin signaling pathway in 3T3-L1 preadipocytes. *Pharm. Biol.* **2013**, *51*, 961–967. [[CrossRef](#)]
17. Zhao, N.; Li, J.; Li, L.; Niu, X.Y.; Jiang, M.; He, X.J.; Bian, Z.X.; Zhang, G.; Lu, A.P. Molecular network-based analysis of guizhi-shaoyao-zhimu decoction, a TCM herbal formula, for treatment of diabetic peripheral neuropathy. *Acta Pharmacol. Sin.* **2015**, *36*, 716–723. [[CrossRef](#)]
18. Shen, F.H.; Yang, W.L.; Zhang, M.J. Clinical Effect of Huangqi Guizhi Wuwu Decoction Modified Combined with Western Medicine in the Treatment of Early Diabetic Foot. *Chin. Foreign Med. Res.* **2021**, *19*, 146–149.
19. Price, D.E.; Alani, S.M.; Carrington, A.; Stickland, M.H.; Wales, J.K. The relationship between peripheral nerve resistance to ischaemia and diabetic control. *J. Neurol. Neurosurg. Psychiatry.* **1987**, *50*, 1671–1673. [[CrossRef](#)]
20. Fen, N. Correlation between glycosylated hemoglobin, C-peptide levels and type 2 diabetes peripheral neuropathy. *Med. J. Chin. People's Health* **2020**, *32*, 134–135.
21. Yu, X.Y.; Zhang, L.; Yang, X.Y.; Huang, H.K.; Huang, Z.G.; Zhang, H.A.; Du, G.H. Salvianolic acid A protects the peripheral nerve function in diabetic rats through regulation of the AMPK-PGC1 α -Sirt3 axis. *Molecules* **2012**, *17*, 11216–11228. [[CrossRef](#)] [[PubMed](#)]
22. Liang, K.; Cui, S.J.; Zhang, Q.; Bi, K.S.; Qian, Z.Z.; Jia, Y. UPLC simultaneous determination of five active components in *Cinnamomi ramulus*. *Chin. J. Chin. Mater. Med.* **2011**, *36*, 3298–3301.

23. Jiang, Y.P.; Liu, R.; Chen, J.J.; Liu, M.H.; Liu, M.; Liu, B.; Yi, L.Z.; Liu, S. Application of multifold characteristic ion filtering combined with statistical analysis for comprehensive profiling of chemical constituents in anti-renal interstitial fibrosis I decoction by ultra-high performance liquid chromatography coupled with hybrid quadrupole-orbitrap high resolution mass spectrometry. *J. Chromatogr. A* **2019**, *1600*, 197–208. [[PubMed](#)]
24. Ye, X.Y.; Wu, J.M.; Yang, J.; Kantawong, F.; Kumsaiyai, W.; Zeng, J. Research progress on chemical constituents of *Gynura divaricate* and mass spectrometry-based fragmentation rules of representative components. *Chin. Tradit. Herb. Drugs* **2021**, *52*, 6687–6700.
25. Zhou, W.W.; Liang, Z.T.; Li, P.; Zhao, Z.Z.; Chen, J. Tissue-specific chemical profiling and quantitative analysis of bioactive components of *Cinnamomum cassia* by combining laser-microdissection with UPLC-Q/TOF-MS. *Chem. Cent J.* **2018**, *12*, 71–80. [[CrossRef](#)] [[PubMed](#)]
26. Cheng, X.; Bi, L.W.; Zeng, W.X.; Zhai, Z.D.; Chen, Y.X.; Zhang, Z.H. Chemical constituents of distillation residues from Cinnamon twigs and leaves by using UHPLC-QTOF-MS. *Chem. Ind. Forest Prod.* **2020**, *40*, 50–60.
27. Kacem, N.; Hay, A.E.; Marston, A.; Zellagui, A.; Rhouati, S.; Hostettmann, K. Antioxidant compounds from Algerian *Convolvulus tricolor* (Convolvulaceae) seed husks. *Nat Prod. Commun.* **2012**, *7*, 873–874. [[CrossRef](#)]
28. Wang, K.H.; Tian, J.Y.; Li, Y.S.; Liu, M.S.; Chao, Y.X.; Cai, Y.; Zeng, G.D.; Fang, Y. Identification of components in *Citri Sarcodactylis* Fructus from different origins via UPLC-Q-Exactive Orbitrap/MS. *ACS Omega.* **2021**, *6*, 17045–17057. [[CrossRef](#)]
29. Weng, Q.Q.; Yang, B.; Li, B.; Deng, A.P.; Zhao, J.C.; Lin, W.M.; Zhan, Z.L.; Huang, L.Q. Analysis of chemical constituents in *Paullinia cupana* dried seeds by UPLC-Q-TOF-MS. *Chin. J. Exp. Tradit. Med. Form.* **2021**, *27*, 68–75.
30. Zeng, W.X.; Cheng, X.; Bi, L.W.; Li, S.N.; Chen, Y.X.; Zhao, Z.D. Effect of biological pretreatment on chemical components from cinnamon cwigs and ceaves. *Chem. Indus Forest Produ.* **2021**, *41*, 101–110.
31. Ma, L.Y.; Wang, Y.M.; Chu, K.; Chen, C.; Wu, S. Determination of phenolic acids and phenol aldehyde compounds in wine by Ultra Performance Liquid Chromatography Tandem Mass Spectrometry. *Chem. Reag.* **2023**, *45*, 141–147.
32. Farag, M.A.; Kabbash, E.M.; Mediani, A.; Döll, S.; Esatbeyoglu, T.; Afifi, S.M. Comparative metabolite fingerprinting of four different cinnamon species analyzed via UPLC-MS and GC-MS and chemometric tools. *Molecules* **2022**, *27*, 2935. [[CrossRef](#)] [[PubMed](#)]
33. He, M.Z.; Jia, J.; Li, J.M.; Wu, B.; Huang, W.P.; Liu, M.; Li, Y.; Yang, S.L.; Ouyang, H.; Feng, Y. Application of characteristic ion filtering with ultra-high performance liquid chromatography quadrupole time of flight tandem mass spectrometry for rapid detection and identification of chemical profiling in *Eucommia ulmoides* Oliv. *J. Chromatogr. A* **2018**, *1554*, 81–91. [[CrossRef](#)] [[PubMed](#)]
34. Abu Bakar, F.I.; Abu Bakar, M.F.; Abdullah, N.; Endrini, S.; Fatmawati, S. Optimization of extraction conditions of phyto-chemical compounds and anti-Gout activity of *euphorbia hirta* L. (Ara Tanah) using response surface methodology and liquid chromatography-Mass spectrometry (LC-MS) analysis. *Evid. Based Complement. Altern. Med.* **2020**, *2020*, 501261–501283. [[CrossRef](#)] [[PubMed](#)]
35. Jia, Q.Q.; Zhang, S.D.; Zhang, H.Y.; Yang, X.J.; Cui, X.L.; Su, Z.H.; Hu, P. A Comparative study on polyphenolic composition of berries from the Tibetan Plateau by UPLC-Q-Orbitrap MS system. *Chem. Biodivers.* **2020**, *17*, 2000033–2000053. [[CrossRef](#)] [[PubMed](#)]
36. Liu, H.X.; Lin, S.; Huang, C.S.; Sun, C.H.; Huang, K.L. Study on chemical component about cinnamomum cassia oil from the different sections of cinnamomum cassia by gas chromatography-mass spectrometry. *Chincondiment* **2011**, *36*, 102–104,110.
37. Chen, P.; Ruan, A.M.; Zhou, J.; Zhang, X.Z.; Wang, Q.F. Exploration on action mechanism of combination of *Ramulus Cinnamoni* and *Radix Paeoniae Alba* in treatment of osteoarthritis based on network pharmacology. *Global Trad. Chin. Med.* **2021**, *14*, 403–410.
38. Yang, Y.L.; Al-Mahdy, D.A.; Wu, M.L.; Zheng, X.T.; Piao, X.H.; Chen, A.L.; Wang, S.M.; Yang, Q.; Ge, Y.W. LC-MS-based identification and antioxidant evaluation of small molecules from the cinnamon oil extraction waste. *Food Chem.* **2022**, *366*, 130576. [[CrossRef](#)]
39. Zhang, F.H.; Wang, Z.M.; Liu, Y.T.; Huang, J.S.; Liang, S.; Wu, H.H.; Xu, Y.T. Bioactivities of serotonin transporter mediate antidepressant effects of *Acorus tatarinowii* Schott. *J. Ethnopharmacol.* **2019**, *241*, 111967–111975. [[CrossRef](#)]
40. Liu, J.Y.; Yang, X.D.; Xu, L.Z.; Yang, S.L. Studies on chemical constituents in dried tender stem of *Cinnamomum cassia*. *Chin. Trad. Herb. Drugs* **2002**, *33*, 681–683.
41. Fu, B.H.; Ji, Y.; Li, J.; Pei, M.; Yang, H.T. Network pharmacology-based mechanism of *Guizhi Mahuang Geban* decoction in treatment of uraemic pruritus. *Trad. Chin. Drug Res. Clinl. Pharm.* **2021**, *32*, 1675–1684.
42. Yoshimura, M.; Ochi, K.; Sekiya, H.; Tamai, E.; Maki, J.; Tada, A.; Sugimoto, N.; Akiyama, H.; Amakura, Y. Identification of characteristic phenolic constituents in Mousouchiku extract used as food additives. *Chem. Pharm. Bull.* **2017**, *65*, 878–882. [[CrossRef](#)] [[PubMed](#)]
43. Chang, S.W.; Lee, J.S.; Lee, J.H.; Kim, J.Y.; Hong, J.K.; Kim, S.K.; Lee, D.H.; Jang, D.S. Aromatic and Aliphatic Apiuronides from the Bark of *Cinnamomum cassia*. *J. Nat. Prod.* **2021**, *84*, 553–561. [[CrossRef](#)] [[PubMed](#)]
44. Caboni, P.; Sarais, G.; Cabras, M.; Angioni, A. Determination of 4-ethylphenol and 4-ethylguaiacol in wines by LC-MS-MS and HPLC-DAD-fluorescence. *J. Agr. Food Chem.* **2007**, *55*, 7288–7293. [[CrossRef](#)]
45. Lam, R.Y.Y.; Lin, Z.X.; Sviderskaya, E.; Cheng, C.H.K. Application of a combined sulphorhodamine B and melanin assay to the evaluation of Chinese medicines and their constituent compounds for hyperpigmentation treatment. *J. Ethnopharmacol.* **2010**, *132*, 274–279. [[CrossRef](#)] [[PubMed](#)]

46. Wang, Y.F.; Harrington, P.B.; Chen, P. Metabolomic profiling and comparison of major cinnamon species using UHPLC-HRMS. *Anal. Bioanal. Chem.* **2020**, *412*, 7669–7681. [[CrossRef](#)] [[PubMed](#)]
47. Han, S.; Karłowicz-Bodalska, K.; Potaczek, P.; Wójcik, A.; Ozimek, L.; Szura, D.; Musiał, W. Identification of unknown impurity of azelaic acid in liposomal formulation assessed by HPLC-ELSD, GC-FID, and GC-MS. *AAPS Pharm. SciTech.* **2014**, *15*, 111–120. [[CrossRef](#)] [[PubMed](#)]
48. Shi, D.H.; Dai, Y.P.; Wang, L.F.; Zhou, Q.; Zhang, X.L.; Zhang, J. Chemical composition analysis of platycladi cacumen before and after being carbonized based on identification by UHPLC-QTOF-MS/MS. *Chin. J. Exp. Tradit. Med. Form.* **2021**, *8*, 107–116.
49. Rius Solé, M.A.; García Regueiro, J.A. Role of 4-phenyl-3-buten-2-one in boar taint: Identification of new compounds related to sensorial descriptors in pig fat. *J. Agr. Food Chem.* **2001**, *49*, 5303–5309. [[CrossRef](#)]
50. Razgonova, M.; Zakharenko, A.; Pikula, K.; Manakov, Y.; Ercisli, S.; Derbush, I.; Kislin, E.; Seryodkin, I.; Sabitov, A.; Kalenik, T.; et al. LC-MS/MS screening of phenolic compounds in wild and cultivated grapes *Vitis amurensis* Rupr. *Molecules* **2021**, *26*, 3650. [[CrossRef](#)]
51. Oliw, E.H.; Garscha, U.; Nilsson, T.; Cristea, M. Payne rearrangement during analysis of epoxyalcohols of linoleic and alpha-linolenic acids by normal phase liquid chromatography with tandem mass spectrometry. *Anal. Biochem.* **2006**, *354*, 111–126. [[CrossRef](#)]
52. Caviglioli, G.; Valeria, P.; Brunella, P.; Sergio, C.; Attilia, A.; Gaetano, B. Identification of degradation products of ibuprofen arising from oxidative and thermal treatments. *J. Pharmaceut. Biomed.* **2002**, *30*, 499–509. [[CrossRef](#)] [[PubMed](#)]
53. Xu, F.; Koch, D.E.; Kong, I.C.; Hunter, R.P.; Bhandari, A. Peroxidase-mediated oxidative coupling of 1-naphthol: Characterization of polymerization products. *Water Res.* **2005**, *39*, 2358–2368. [[CrossRef](#)] [[PubMed](#)]
54. Xu, C.J.; Liang, Y.Z.; Song, Y.Q.; Li, J.S. Resolution of the essential constituents of *Ramulus cinnamomi* by an evolving chemometric approach. *Fresen J. Anal. Chem.* **2001**, *371*, 331–336. [[CrossRef](#)] [[PubMed](#)]
55. Yongram, C.; Sungthong, B.; Puthongking, P.; Weerapreeyakul, N. Chemical composition, antioxidant and cytotoxicity activities of leaves, bark, twigs and oleo-resin of dipterocarpus alatus. *Molecules* **2019**, *24*, 3083. [[CrossRef](#)] [[PubMed](#)]
56. Mueller, M.; Beck, V.; Jungbauer, A. PPAR α activation by culinary herbs and spices. *Planta Med.* **2011**, *77*, 497–504. [[CrossRef](#)] [[PubMed](#)]
57. Guo, Y.P.; Yang, H.; Wang, Y.L.; Chen, X.X.; Zhang, K.; Wang, Y.L.; Sun, Y.F.; Huang, J.; Yang, L.; Wang, J.H. Determination of Flavonoids Compounds of Three Species and Different Harvesting Periods in *Crataegi folium* Based on LC-MS/MS. *Molecules* **2021**, *26*, 1602. [[CrossRef](#)]
58. Liang, H.B.; Jiang, Y.J.; Yuan, X.M.; Yao, J.C.; Qiu, R.Y.; Yang, M.; Zhang, G.M.; Li, F. Chemical constituents of Jingfang granules based on GC-MS and UPLC-Q Exactive MS. *Chin. Tradit. Herb. Drugs* **2022**, *53*, 1697–1708.
59. Qiao, X.; Li, R.; Song, W.; Miao, W.J.; Liu, J.; Chen, H.B.; Guo, D.A.; Ye, M. A targeted strategy to analyze untargeted mass spectral data: Rapid chemical profiling of *Scutellaria baicalensis* using ultra-high performance liquid chromatography coupled with hybrid quadrupole orbitrap mass spectrometry and key ion filtering. *J. Chromatogr. A* **2016**, *1441*, 83–95. [[CrossRef](#)]
60. Sang, Q.N.; Jia, Q.Q.; Zhang, H.Y.; Lin, C.H.; Zhao, X.D.; Zhang, M.; Wang, Y.R.; Hu, P. Chemical profiling and quality evaluation of *Zhishi-Xiebai-Guizhi* decoction by UPLC-Q-TOF-MS and UPLC fingerprint. *Pharm. Biomed. Anal.* **2021**, *194*, 113771. [[CrossRef](#)]
61. Yang, W.; Ye, M.; Liu, M.; Kong, D.Z.; Shi, R.A.; Shi, X.W.; Zhang, K.R.; Wang, Q.; Zhang, L.T. Practical strategy for the characterization of coumarins in *Radix Glehniae* by liquid chromatography coupled with triple quadrupole-linear ion trap mass spectrometry. *J. Chromatogr. A* **2010**, *1217*, 4587–4600. [[CrossRef](#)]
62. Yang, H.; Jiang, B.; Reynertson, K.A.; Basile, M.J.; Kennelly, E.J. Comparative analyses of bioactive *Mammea* coumarins from seven parts of *Mammea americana* by HPLC-PDA with LC-MS. *J. Agric. Food Chem.* **2006**, *54*, 4114–4412. [[CrossRef](#)] [[PubMed](#)]
63. Liu, C.; Long, H.L.; Wu, X.D.; Hou, J.J.; Gao, L.; Yao, S.A.; Lei, M.; Zhang, Z.J.; Gao, D.A.; Wu, W.Y. Quantitative and fingerprint analysis of proanthocyanidins and phenylpropanoids in *Cinnamomum verum* bark, *Cinnamomum cassia* bark, and *Cassia* twig by UPLC combined with chemometrics. *Eur. Food Res. Technol.* **2021**, *247*, 2687–2698. [[CrossRef](#)]
64. Wang, S.H.; Huang, W.L.; Chen, Q.S.; Zeng, L.; Zeng, F.J. Inhibition of rutin and quercetin on α -glycosidase. *Chin. Brew Maga* **2012**, *31*, 133–135.
65. Li, Y.H.; Wei, J.C.; Liang, J.L.; Huang, Q.X.; Huang, R.S.; Lei, P.L. Simultaneous determination of coumarin, cinnamic acid and cinnamaldehyde in *folium cinnamomicum* by HPLC. *Chin. J. Trad. Chin. Med.* **2020**, *38*, 54–57.
66. Kim, C.; Lee, J.H.; Kim, W.J.; Li, D.X.; Kim, Y.S.; Lee, K.J.; Kim, S.K. The suppressive effects of cinnamomi cortex and its phytochemical coumarin on oxaliplatin-induced neuropathic cold allodynia in rats. *Molecules* **2016**, *21*, 1253. [[CrossRef](#)]
67. Chen, K.K.; Liu, J.; Ma, Z.C.; Duan, F.P.; Guo, Z.H.; Xiao, H.B. Rapid identification of chemical constituents of *Rhodiola crenulata* using liquid chromatography-mass spectrometry pseudotargeted analysis. *J. Sep. Sci.* **2021**, *44*, 3747–3776. [[CrossRef](#)]
68. Goodner, K.L.; Rouseff, R.L. Using an ion-trap MS sensor to differentiate and identify individual components in grapefruit juice headspace volatiles. *J. Agric. Food Chem.* **2001**, *49*, 250–253. [[CrossRef](#)]
69. Chandra, P.; Rathore, A.S.; Kay, K.L.; Everhart, J.L.; Curtis, P.; Burton-Freeman, B.; Cassidy, A.; Kay, C.D. Contribution of berry polyphenols to the human metabolome. *Molecules* **2019**, *24*, 4220. [[CrossRef](#)]
70. Zhang, W.D.; Wang, X.J.; Zhou, S.Y.; Gu, Y.; Wang, R.; Zhang, T.L.; Gan, H.Q. Determination of free and glucuronidated kaempferol in rat plasma by LC-MS/MS: Application to pharmacokinetic study. *J. Chromatogr. B* **2010**, *878*, 2137–2140. [[CrossRef](#)]
71. Hu, J.; Zhao, J.P.; Khan, S.I.; Liu, Q.; Liu, Y.; Ali, Z.; Li, X.C.; Zhang, S.H.; Cai, X.; Huang, H.Y.; et al. Antioxidant neolignan and phenolic glucosides from the fruit of *Euterpe oleracea*. *Fitoterapia* **2014**, *99*, 178–183. [[CrossRef](#)]

72. Kim, S.E.; Lee, J.; An, J.U.; Kim, T.H.; Oh, C.W.; Ko, Y.J.; Krishnan, M.; Choi, J.; Yoon, D.Y.; Kim, Y.; et al. Regioselectivity of an arachidonate 9S-lipoxygenase from *Sphingopyxis macrogoltabida* that biosynthesizes 9S,15S- and 11S,17S-dihydroxy fatty acids from C20 and C22 polyunsaturated fatty acids. *BBA-Mol. Cell Biol. Lipids* **2022**, *1867*, 159091. [[CrossRef](#)] [[PubMed](#)]
73. Kenari, F.; Molnár, S.; Perjési, P. Reaction of Chalcones with Cellular Thiols. The Effect of the 4-Substitution of Chalcones and Protonation State of the Thiols on the Addition Process. Diastereoselective Thiol Addition. *Molecules* **2021**, *26*, 4332. [[CrossRef](#)] [[PubMed](#)]

Disclaimer/Publisher's Note: The statements, opinions and data contained in all publications are solely those of the individual author(s) and contributor(s) and not of MDPI and/or the editor(s). MDPI and/or the editor(s) disclaim responsibility for any injury to people or property resulting from any ideas, methods, instructions or products referred to in the content.